Response to Referees

Manuscript acp-2016-753

Characterization of gas-phase organics using proton transfer reaction time-of-flight mass spectrometry: fresh and aged residential wood combustion emissions

Emily A. Bruns, Jay G. Slowik, Imad El Haddad, Dogushan Kilic, Felix Klein, Josef Dommen, Brice Temime-Roussel, Nicolas Marchand, Urs Baltensperger and André S. H. Prévôt

We thank the Referees for the comments and we have incorporated the feedback to improve the manuscript. We have copied the remarks of each Referee in *black italics* and our responses are given in regular black font. Manuscript text including revisions is given in regular blue font.

Anonymous Referee #1

Bruns et al. describe controlled laboratory measurements of fresh and aged emissions from the residential combustion of beech wood. The authors generated these emissions using a commercial wood burner. Using a high-resolution proton transfer reaction time-of-flight mass spectrometer, the authors measured primary VOC emissions under stable flaming conditions. For aging experiments, the emissions were directed into a Teflon chamber and oxidized by OH radicals generated from the photolysis of nitrous acid. Primary emissions exhibited significant enhancements of oxygenated species (particularly acids) and aromatic compounds. The emissions of typical nitrogen-containing biomass burning markers, such as acetonitrile, were significantly lower than those observed from open burning. During aging experiments, the authors observed significant consumption of NMOG mass. Certain species, such as formic acid and phthalic anhydride, showed significant enhancements. Acetic acid, however, exhibited no net increase, which the authors attribute to the balancing of secondary production + OH consumption.

The manuscript is written clearly and the contents are well organized. The study is interesting, well executed, and the results provide insights into the chemical evolution of wood smoke, which is poorly constrained yet important for regional air quality. My primary comments pertain to the conclusions drawn about secondary NMOG and the observations of low acetonitrile. In particular, I believe the authors should provide an expanded discussion (and potentially further insights) into the variability of NMOG oxidation products (see point 2). Upon addressing these comments, I recommend the manuscript for publication.

We have addressed the Referee's comments as detailed below, including modifying the manuscript to provide an expanded discussion and further insights into the variability of NMOG oxidation products and observations of low acetonitrile emissions.

Comments

1) Secondary NMOG:
The authors discuss a number of processes that could affect the observed net decrease in NMOG mass, including gas-to-particle partitioning and conversion of gasphase species to those that

1

cannot be detected by the PTR-ToF-MS. However, the authors do not include a discussion about vapor-phase wall loss. Bian et al. (2015) simulated the loss of primary biomass burning emissions to a Teflon chamber and demonstrated that wall loss can significantly affect both particle and gas-phase organics. In the average simulation, ~75% of gas-phase vapors were lost to the chamber. Stockwell et al. (2014) observed losses of biomass burning organic compounds (including acetic acid) to surfaces at very different rates. Can the authors estimate and/or discuss the impact of wall loss and potentially provide uncertainties to the 5 – 30% loss in NMOG mass?

NMOG wall losses were inferred by monitoring NMOG concentrations prior to initiating photochemistry and by assessing the smog chamber conditions affecting loss rates during aging as detailed by Zhang et al. (2014 and 2015) (Zhang, X., Cappa, C.D., Jathar, S.H., McVay, R.C., Ensberg, J.J., Kleeman, M.J. and Seinfeld, J.H.: Influence of vapor wall loss in laboratory chambers on yields of secondary organic aerosol, Proceedings of the National Academy of Sciences 111, 5802–5807, 2014; Zhang, X., Schwantes, R. H., McVay, R. C., Lignell, H., Coggon, M. M., Flagan, R. C., and Seinfeld, J. H.: Vapor wall deposition in Teflon chambers, Atmos. Chem. Phys., 15, 4197–4214, 2015). Bian et al. (2015) found that the concentration of gas-phase emissions generated during open burning decreased by 86% due to vapor wall losses in a dark chamber using best estimate parameters in a model. When using effective wall saturation concentrations based on the study of Zhang et al., Bian et al. (2015) found that the net vapor loss to the walls decreased by 65% compared to the best estimate. While open biomass burning emission profiles share similarities with residential burning emissions, differences can be large (e.g., see response below regarding emission of nitrogen-containing species), making it difficult to apply the findings of Bian et al. (2015) to residential burning, particularly as vapor losses are very sensitive to the model parameters. We think more investigation of residential wood combustion emissions is needed to be able to apply meaningful uncertainties on the loss in NMOG mass in the current study, but we agree with the Referee that a discussion of potential NMOG wall losses is needed in the manuscript and we have modified the text as follows (Pages 16-17, lines 349-359): "In addition to gas to particle phase partitioning and formation of gas-phase species not quantified here, a decrease in NMOG mass with aging could also be due to losses of gas-phase species to the chamber walls (Zhang et al., 2014; Bian et al., 2015). Measurements of NMOGs in the chamber prior to aging are stable, indicating that the chamber walls are not a sink for NMOGs, but rather that NMOGs are in equilibrium with the chamber walls, particles and the gas phase. Zhang et al. (2014) show that the rate of NMOG wall loss is proportional to seed aerosol concentration and OH concentration, both of which were relatively high in the current experiments (Table S1; OH concentrations were ~$1.4x10^7$ molec cm^{-3}). Under these experimental conditions, NMOG wall losses are not expected to be large. However, future studies are needed to provide insight into vapor wall loss of residential wood combustion emissions during aging."

In addition to wall loss, I think the authors should also discuss the variability of secondary organic production. This discussion is provided for primary emissions (Section 3.2), but few insights are drawn from the variability of oxidation products. There are significant differences between the trends observed during Expts. 2,3 and those observed during Expts. 1,4,5 (Figs. 4 and 5). For example, acids and O-containing compounds show a general increase in Expts 1,4,5, but a decrease in Expts 2,3. It is notable that the initial NMOG distributions in Expts 1,4,5

contain a higher fraction of aromatic and oxygenated aromatics. Could it be that these compounds are a significant source of secondary acids and O-containing compounds? It should also be noted that other compounds not measured by proton-transfer could also impact these trends (e.g. ethylene). This variability is quite interesting and a discussion pertaining to these differences may help in understanding the variability of OVOC formation in open burning (e.g. de Gouw et al. 2006 vs Yokelson et al. 2003).

We agree with the Referee that more discussion on the variability of the aged emission profiles is needed and we have added a new section in the manuscript to address this topic (3.5 Aged emission variability). We have also included the discussion on variability of SOA formation potential in this section. The text has been modified as follows (Pages 19-20, section 3.5): "As described above, the primary emission profiles, as well as total NMOG mass emitted, vary considerably for experiments 2 and 3 compared to experiments 1, 4 and 5, with much higher total NMOG emissions in experiments 2 and 3. It is expected that the aged emission profiles also exhibit variability based on the primary emissions. Total acid and O-containing species decrease with aging in experiments 2 and 3, in contrast to experiments 1, 4 and 5, where these classes increase with aging (Figure 4). Formic acid shows the largest increase with aging in all experiments (~190-480 mg kg^{-1} relative to the primary EF, Figure 5), however, in experiments 1, 4 and 5, this increase contributes much more to the total acid mass as the total acid mass is ~5-15 times lower compared to experiments 2 and 3. An analogous case occurs for maleic anhydride for the O-containing class of compounds. As formic acid and maleic anhydride are formed from the oxidation of aromatic compounds (Bandow et al., 1985; Sato et al., 2007; Praplan et al., 2014), among others, a higher fraction of aromatic species to the total NMOG emissions will contribute to increases in acid and O-containing NMOGs. Inclusion of NMOGs not quantified by PTR-ToF-MS could impact the trends observed in Figure 4."

2) Acetonitrile
In Section 3.3, the authors discuss the variability of acetonitrile. The authors attribute the observations of low acetonitrile to burning conditions. While burning efficiency and O2 fraction certainly affect NMOG emissions, very recent work demonstrates that fuel composition plays a major role in the variability of nitrogen-containing VOCs (Coggon et al. 2016). In that study, the authors show that wood (low nitrogen content) emits a significantly lower fraction of nitrogen-containing VOCs than other tree components, such as leaves and boughs (high nitrogen content).

Given this new work, the authors should also discuss the effects of fuel composition. Assuming that the beech wood is free of stems, twigs, or leaves, then it is likely that low acetonitrile emissions result from the combustion of low nitrogen-containing fuel.
Have the authors also considered looking at the emissions of other nitrogen-containing NMOGs that are sensitive to proton-transfer, such as acrylonitrile or HNCO? These species would also likely exhibit lower EFs compared to open burning of fuels with higher nitrogen content.

We thank the Referee for bringing the recent work of Coggon et al. (2016) to our attention. The beech wood in our study was free of stems, twigs, leaves and bark, and based on the work of Coggon et al. (2016), we therefore expect that a relatively low fraction of the total NMOGs was N-containing compared to burning of biomass containing leaves, etc. This fact may explain the relatively low acetonitrile emissions in our study compared to open biomass burning, where

leaves, bark, etc. are typically present. The primary emission factors of C_3H_3N and HNCO ranged in our study from 3.6-6.4 mg kg^{-1} and BLD (<tens of pptv)-11 mg kg^{-1}, respectively. Emission factors of acrylonitrile (C_3H_3N) observed during open burning are higher than those observed in the current study (~10-90 mg kg^{-1}, Akagi et al., 2013), as expected based on the lower acetonitrile emission factors observed in the current study and the findings of Coggon et al., 2016.

We have expanded the discussion of acetonitrile emissions to include this information (Page 14, lines 288-300): "In agreement with the current study, ambient measurements of acetonitrile made in Colorado (USA) were not associated with fresh residential burning emissions (Coggon et al., 2016). Lower ambient measurements of nitrogen-containing NMOGs (including acetonitrile) during residential burning compared to open burning were attributed to the generally lower nitrogen content in fuels burned residentially (Coggon et al., 2016). Lower nitrogen content of the fuel is likely a contributor to the relatively low acetonitrile emissions in the current study.

The primary emission factors of other nitrogenated species, such as C_3H_3N (likely corresponding to acrylonitrile) and HNCO ranged in our study from 3.6-6.4 mg kg^{-1} and BDL-11 mg kg^{-1}, respectively. Emission factors of C_3H_3N in the current study are lower than those observed during open burning (e.g., ~10-90 mg kg^{-1} (Akagi et al., 2013)), as expected based on the lower acetonitrile emission factors observed in the current study and the findings of Coggon et al. (2016)."

Other Comments

Line 45: The descriptor "residential wood combustion" is unclear. Other studies have investigated the emissions from fuels typically burned in stoves (e.g. Douglas Fir, Stockwell 2015). To avoid confusion, please specify that you are speciating wood combustion emissions from commercial stoves.

The text has been modified as follows to specify that wood combustion emissions were speciated from commercial stoves (Page 3, lines 44-46): "Although two studies have speciated a large fraction of the NMOG mass emitted during residential wood combustion in commercial burners…"

Line 76: Please provide more details about the burner. Is the appliance fitted with a catalyst or secondary combustion zone? A description or schematic would be helpful for other researchers studying the emissions from other wood burners.

The burner was manufactured in 2009 and is not fitted with a catalyst or other emission control device. There is no secondary combustion zone. A photograph of the burner was added to the SI (new Figure S1) and a description of the burner was added to the main text (Page 4, lines 77-78): "… a residential wood burner (Figure S1; single combustion chamber, operated in single batch mode; Avant, 2009, Attika)…"

Line 90-91 What kind of lights are used to photolyze HONO? Can the authors provide flux measurements (or cite a source containing this information)?

In the chamber, HONO is photolyzed using 40 UV lights of 90-100 W (Cleo Performance, Philips) (Page 5, lines 98-99). Emission spectra of these lights, as well as inferred NO_2 amd HONO photolysis rates for a similar set-up to the current study, can be found in Platt et al. (2013): Secondary organic aerosol formation from gasoline vehicle emissions in a new mobile environmental reaction chamber, Atmos. Chem. Phys. 13, 9141-9158, 2013. This reference has been added to the manuscript.

Line 91: How do these levels of NOx compare to those from other biomass burning sources? NOx will also depend on fuel composition (e.g. Burling et al. 2010). Furthermore, how do NOx levels change after initiating the photolysis of HONO? Did the authors also measure ozone? If so, how much was formed as a result of photochemical processing? I believe these conditions are important to discuss, especially for future studies focused on biomass burning aging.

For NO_x, the primary EFs ranged from ~0.5-0.7 g kg^{-1} (~160-350 ppbv in the chamber (mainly NO); no primary measurement available for experiment 1), which are much lower than literature for open burning (Stockwell et al., 2015 from open biomass burning of ponderosa pine (~2-5 g kg^{-1}) and black spruce (4-5 g kg^{-1})). Lower NO_x (and N-containing NMOGs) EFs are expected due to the lower nitrogen content of the fuel used compared to open burning (Coggon et al., 2016). Upon aging, NO_x increased to ~250-380 ppbv after reaching OH exposures of ~(4.5-5.5)$\times10^7$ molec cm^{-3} h, due to HONO photolysis. We have to note that NO_x was measured using a chemiluminescence analyzer, and therefore the aforementioned concentrations should be considered as upper estimates, as the measurements are affected by NO_y species (especially nitric acid).

Considering these high NO_x values and the levels of measured reactive NMOGs in the beginning of the experiments (NMOG/NO_x ratios of ~1-10), O_3 production is favored. For these experiments, we did not measure O_3 concentrations. However, previous measurements conducted under similar conditions indicate an initial O_3 production with aging. After an initial increase, O_3 concentrations significantly decrease due to the decrease of NMOG/NO_x ratios (NMOG consumption and NO_x increase with HONO photolysis).

The primary NO_x values were added to the manuscript in a new table in the SI (Table S1), which includes other experimental parameters, as suggested by the other Referee. The following was added to the main text (Page 5, line 88): "Experimental parameters and primary emission values are summarized in Table S1." and (Page 5, lines 94-96): "Levels of NO_x in the chamber prior to aging range from ~160-350 ppbv and increases to ~250-380 ppbv after reaching OH exposures of ~(4.5-5.5)$\times10^7$ molec cm^{-3} h (NO_x data unavailable for experiment 1)."

Section 3.2. The discussion about burn variability is much appreciated. Can the authors propose reasons for these differences? The tight reproducibility of MCE makes me think it's not necessarily burning efficiency. Could there also be variability in how the burner operates that could lead to these differences (e.g. temperature)? Syc et al. observed significantly different emission factors of PAHs from a commercial burner when burning lignite at various temperatures. Hansson et al. (2004) observed differences in nitrogen NMOG distributions as a function of temperature for the pyrolysis of bark and other biomass sources. I would imagine that similar effects could be true for the combustion of beech wood.

We agree with the Referee that MCE, which is very similar in all experiments, is unlikely to be the cause of the difference in emission profiles between the experiments. As great care was taken to replicate each burn as closely as possible (e.g., similar starting wood mass, number of logs/kindling pieces and wood arrangement prior to ignition) and experimental conditions (e.g., dilution factors), there is no obvious explanation for the inter-experimental variability. The burner was housed in an uninsulated building and, as suggested, the variability could be due to effects of differences in outdoor temperature on the burner which would influence the combustion rate. Each fire was allowed to burn for 15-20 minutes prior to injecting emissions into the smog chamber, which allowed the burner to warm up, however, we did not make temperature measurements in the burner or chimney and temperature differences may have remained. The discussion on inter-burn variability was expanded to include these points (Page 13, lines 262-266): "The burner is housed in an uninsulated building and the emission profile variability could be due to effects of outdoor temperature variability on the burner. For example, emission profiles from burning lignite and pyrolysis of bark and other biomass sources have been shown to vary with burn temperature (Hansson et al., 2004; Šyc et al., 2011)."

Fig. 4: I assume that each panel is the temporal evolution of gas-phase species from each aging experiment. Is that correct? Please clarify.

Each panel corresponds to the temporal evolution for a single experiment. The figure legend has been modified, "…Temporal evolution of gas-phase species categorized by functional group throughout aging in the smog chamber for experiments 1-5 (a-e)."

References:
Bian, Q., May, A. A., Kreidenweis, S. M., and Pierce, J. R.: Investigation of particle and vapor wall-loss effects on controlled wood-smoke smog-chamber experiments, Atmos. Chem. Phys., 15, 11027-11045, doi:10.5194/acp-15-11027-2015, 2015.

Coggon, M.M., Veres, P.R., Yuan, B., Koss, A., Warneke, C., Gilman, J.B., Lerner, B., Peischl, J., Aikin, K., Stockwell, C., Hatch, L., Ryerson, T.B., Roberts, J.M., Yokelson, R., and de Gouw, J.: Emissions of nitrogen-containing organic compounds from the burning of herbaceous and arboraceous biomass: fuel composition dependence and the variability of commonly used nitrile tracers, Geophys. Res. Lett., 43, doi: 10.1002/2016GL070562, 2016.

Hansson, K., Samuelsson, J., Tullin, C., and Amand, L.: Formation of HNCO, HCN, and NH3 from the pyrolysis of bark and nitrogen-containing model compounds, Combustion and Flame, 137 (3), 265-277, doi: 10.1016/j.combustflame.2004.01.005, 2004.

Šyc, M., Horák, J., Hopan, F., Krpec, K., Tomšej, T., Ocelka, T., and Pekárek.V, Effect of Fuels and Domestic Heating Appliance Types on Emission Factors of Selected Organic Pollutants, Environ. Sci. Technol., 45 (21), 9427-9434, doi: 10.1021/es2017945, 2011.

Anonymous Referee #2

This paper presents measurements of gas-phase species emitted from combustion of beech in a 'modern' residential heating stove in both fresh and aged states. Five replicate laboratory experiments were conducted in which emissions from a steady flaming combustion were sampled into a laboratory smog chamber, from which there were sampled for both a primary characterization period and during oxidation by OH formed via HONO photolysis. The use of replicate experiments is useful, as it assesses the extent to which emissions vary even within narrowly controlled circumstances – as it turns out, quite a bit. Interestingly, many of the emissions of concern (CO, OA, BC) are quite consistent across tests, as is the SOA produced during aging. In contrast, the composition and emission factors of NMOG varied substantially, with two tests having markedly different NMOG emissions. The evolution of NMOG is described in which many identified species show the expected decay with OH oxidation, while other species (acids, other O-containing species) showed enhancement.

This paper is clearly written and the measurements and analysis appear to be of high quality. This topic is of great interest to the readership of ACP as it provides important insights into the composition and evolution of an important class of biomass burning emissions. Below I have highlighted several points that would like to see addressed in revisions. The main focus of my comments is on the difference between the two sets of experiments – I would like to see a bit more discussion of the conditions that lead to these differences and how the two 'anomalous' experiments (#2, #3) differ from the others. This seems to be a key point, and while the differences are discussed, there's little investigation of what might have influenced this difference. For example, the fuel consumed was nearly half during these experiments than the others, why? One general comment is that I was really required to read the other Bruns et al. 2016 paper in order to understand and interpret these results. While I understand that the authors split these aspects of the reporting of the project to avoid a cumbersome manuscript, I would like to see this one 'stand alone'. So, at the least I would suggest that a table of basic test parameters (like Table 1 in Bruns et al 2016) be included, perhaps in the SI. Another general comment is that there is a bit of an over-emphasis on differences between results observed here (one fuel, one combustion condition) and observations more generally. In most cases, these comparisons are appropriately caveated, but in some cases the generalizations are a bit sweeping (e.g. Line 283) – I ask the authors to give this a once over to ensure that these results, while certainly providing key insights and data, are not over-extrapolated. Finally, I second many of the concerns/questions of the first referee.

Once these general and specific points have been addressed, I recommend the manuscript for publication in ACP.

We have expanded the discussion on the differences between the two sets of experiments (2 and 3 vs 1, 4 and 5) as described in detail below. We agree that this manuscript should 'stand-alone' and have taken the suggestion of the Referee to add a table with the experimental parameters to the SI (new Table S1). We have also modified the text to ensure the insights from these data are not over-extrapolated, as described below. The responses to the concerns/questions of the first Referee are detailed above.

Specific points
I am a bit confused by Table 2 – this indicates acetonitrile as the only N-containing species, but EF of acetonitrile is ~10 times lower than that for N-containing species? Is the rest of this mass contributed by un-identified compounds? It also doesn't seem as if N-containing species contribute 20-30 mg/kg to NMOG mass on Figure 1, but it would be hard to see there. N-containing species were higher for Expts. 2-3, but aerosol-phase nitrate was substantially lower (even accounting for lower fuel consumption) (Bruns et al. 2016). Were there any other notable differences? E.g. NOx levels? Have you examined secondary nitrate formation during aging?

There are 14 N-containing species which contribute to this category and it is correct that 13 of these N-containing species have not been structurally assigned (the exception is acetonitrile). One reason for the lack of assignments is a scarcity of published data on N-containing emissions from residential wood combustion compared to emissions of other classes of compounds. However, an educated guess can be made about several of these compounds based on reasonable structures (e.g., C_3H_3N likely corresponds to acrylonitrile, as discussed in the response to the other Referee). A brief discussion and the range of emission factors observed for C_3H_3N and HNCO (in the O- and N-containing category), two compounds of interest in open biomass burning emissions, have been added to the text (Page 14, lines 288-300; see response to other Referee). Future work to identify more N-containing species emitted during residential wood combustion would be informative, similar to the recent work on identifying N-containing emissions from open biomass burning (i.e., Coggon et al., 2016, Stockwell et al., 2015). The majority of the mass contributing to the N-containing class is distributed among several compounds and the total mass of N-containing species is the lowest of all classes, which is likely why it is difficult to see these individual N-containing species in Figure 1.

N-containing species were higher and aerosol phase nitrate lower in experiments 2 and 3 compared to experiments 1, 4 and 5, however, there was no notable difference in NO_x emissions between experiments 2 and 3 (~0.5 and 0.7 g kg^{-1}, respectively) compared to experiments 1, 4 and 5 (~0.5 and 0.6 g kg^{-1}, respectively; NO_x data not available for experiment 1). With aging, particulate nitrate (NO_3) showed varied behavior; however, there is no trend between experiments 2 and 3 compared to experiments 1, 4 and 5. After correction for wall losses, NO_3 remains stable in experiment 1, NO_3 increases by ~15% of its primary value during initial aging and then remains stable in experiment 2, NO_3 decreases by ~10% of its primary value during initial aging and then remains stable in experiment 3, and NO_3 increases by ~15% of its primary value in experiments 4 and 5 and then slowly decreases with further aging. AMS measurements of NO_3 includes inorganic and organic species; however, characterization, including quantification, of organic nitrate species is challenging using aerosol mass spectrometry and more work is needed to investigate particulate organic nitrates from residential wood combustion. The presence of bark, twigs and leaves have recently been shown to influence the emission of N-containing species during burning (Coggon et al., 2016), however, no difference in fuel composition is expected between the experiments as all bark and twigs were removed prior to combustion. As described above in a response to other Referee, differences in emission profiles may have been due to differences in ambient temperature effecting burner operation leading to differences in combustion rates.

L255 – Figure 2 is just mentioned here, and this could bear a bit more discussion and the differences between experiments discussed a bit further. One thing that stands out about these two experiments (2, 3) is that the CO2 loading in the chamber was substantially (almost half) lower than the other three experiments (despite the fact that the MCEs and many other quantities are essentially the same. If the injection time and dilution conditions were the same, this suggests that perhaps the combustion rate was lower (which would probably be indicated by lower flue temperature). Are there any other contextual or operational details that were different?

This point was raised by the other Referee as well. The MCE, which is very similar in all experiments, is unlikely to be the cause of the difference in emission profiles between the experiments. As great care was taken to replicate each burn as closely as possible (e.g., similar starting wood mass, number of logs/kindling pieces and wood arrangement prior to ignition) and experimental conditions (e.g., dilution factors), there is no obvious explanation for the inter-experimental variability. The burner was housed in an uninsulated building and, as suggested by the both Referee, the variability could be due to effects of differences in outdoor temperature on the burner and chimney which would reduce the combustion rate. Each fire was allowed to burn for 15-20 minutes prior to injecting emissions into the smog chamber, which allowed the burner to warm up, however, we did not make temperature measurements in the burner or chimney and temperature differences may have remained. The discussion on inter-burn variability was expanded to include these points (Page 13, lines 262-266): "The burner is housed in an uninsulated building and the emission profile variability could be due to effects of outdoor temperature variability on the burner. For example, emission profiles from burning lignite and pyrolysis of bark and other biomass sources have been shown to vary with burn temperature (Hansson et al., 2004; Šyc et al., 2011)."

L283 – This is too broad/definitive of a statement to make based on the narrow set of conditions tested here.

The text has been modified as follows (Page 14, lines 304-306): "…making acetonitrile a poor marker for residential wood combustion under these burning conditions. Coggon et al. (2016) concluded that acetonitrile may not be a good tracer for residential burning in urban areas."

L317-319 – It would be useful/instructive to attempt a mass balance on the NMOG and SOA loadings to estimate how much of the measured NMOG may be ending up in the condensed phase in your experiments.

The work detailed in our previous publication on these experiments provides the first quantitative closure of the mass balance of the gas-phase species contributing to SOA (Bruns et al., 2016). We determined that the conversion of NMOGs traditionally included in models to SOA account for only ~3-27% of the observed SOA, whereas ~84-116% of the SOA can be explained by inclusion of non-traditional precursors, including naphthalene and phenol. The text was modified as follows (Page 16, lines 343-346): "Previous investigation of these experiments determined that the conversion of NMOGs traditionally included in models to SOA accounts for only ~3-27% of the observed SOA, whereas ~84-116% of the SOA is explained by inclusion of non-traditional precursors, including naphthalene and phenol (Bruns et al., 2016)."

9

L358 – Were terpenes actually quantified? I don't expect much from birch wood, but if you measured them (or found them BDL) this should be noted.

As expected from previous studies (e.g., Schauer et al., 2001), monoterpenes were below the detection limit in all experiments. Isoprene emissions (Table 2) were also relatively low, although above the detection limit. This information has been added to the manuscript (Page 18, lines 394-395): "Monoterpene concentrations are below the detection limit in all experiments and isoprene emissions are relatively low (Table 2)."

L362 – 'Good agreement' is a bit vague, there is not-great agreement in panels c) and f). Could this indicate possibly misattribution of these compounds? For this figure, it would be helpful to show smoothed data (and probably a log y-axis) to make this a bit more readable.

We have modified the Figure (now Figure S3) to show the smoothed data (10 s data smoothed to 5 min moving average) to improve readability. We have also added some additional discussion of this Figure to address the Referee's comments that the agreement is better for some compounds (i.e., panels a, b, c, e, g, h) compared to others (i.e., panels d, f and i) (Page 19, lines 400-408): "There is generally good agreement between the observed and calculated decay for each compound which supports the structural assignment of each ion. For 2-methoxyphenol and 2,6-dimethoxyphenol (Figure S3 f and i, respectively), the agreement between the observed and calculated decays is not as good as for the other compounds, with slower decays than predicted. This discrepancy may be due to fragmentation of related compounds to form 2-methoxyphenol and 2,6-dimethoxyphenol in the instrument or formation of these compounds in the chamber during oxidation. For *o*-benzenediol, the decays are initially faster than expected and then become slower with increased aging, possibly due to the presence of isomers with different reaction rates with respect to OH."

L365-370 - Somewhat confusing lead-in to discussion of Figure 3, as discussion emphasizes differences between experiments and this figure shows averages across all experiments - may make sense to just discuss this result then discuss inter-experiment differences (using Fig. 2)

We agree with the Referee and have introduced Figure 3 in the preceding paragraph and then discussed the inter-experiment differences on SOA formation potential using Figure 2 in the next paragraph (Pages 18-20, lines 396-433): "We have previously identified the compounds contributing to the majority of the SOA formed during these experiments (Bruns et al., 2016). The average EF for each of these species is shown in Figure 3. Figure S3 shows the observed decay of the SOA precursors contributing the most to SOA formation during aging in the chamber compared to the expected decay based on the OH concentration in the chamber and the reaction rate with respect to OH. There is generally good agreement between the observed and calculated decay for each compound which supports the structural assignment of each ion. For 2-methoxyphenol and 2,6-dimethoxyphenol (Figure S3 f and i, respectively), the agreement between the observed and calculated decays is not as good as for the other compounds, with slower decays than predicted. This discrepancy may be due to fragmentation of related compounds to form 2-methoxyphenol and 2,6-dimethoxyphenol in the instrument or formation of these compounds in the chamber during oxidation. For *o*-benzenediol, the decays are initially faster than expected and then become slower with increased aging, possibly due to the presence of isomers with different reaction rates with respect to OH.

As described above, the overall primary emission profiles, as well as total NMOG emissions, vary considerably for experiments 2 and 3 compared to experiments 1, 4 and 5, with considerably higher total NMOG emissions in experiments 2 and 3. To determine the impact of the high NMOG emission experiments (2 and 3) compared to the lower NMOG emission experiments (1, 4 and 5) on SOA formation potential, individual SOA precursors with published SOA yields are investigated. The SOA formation potential for each of these 18 compounds is determined as the product of the primary EF and the best estimate SOA yield determined from the literature, as determined previously (Bruns et al., 2016). The total SOA formation potential for each experiment is taken as the sum of the individual SOA formation potentials. Interestingly, the SOA formation potential is similar in all experiments and the average enhancement of SOA formation potential in experiments 2 and 3 compared to the average of experiments 1, 4 and 5 is insignificant (Figure 2), despite the considerably different total NMOG EFs."

References

Bruns, E. A., El Haddad, I., Slowik, J. G., Kilic, D., Klein, F., Baltensperger, U., and Prévôt, A. S. H. (2016). "Identification of significant precursor gases of secondary organic aerosols from residential wood combustion." Scientific Reports, 6, 27881.

Characterization of gas-phase organics using proton transfer reaction time-of-flight mass spectrometry: fresh and aged residential wood combustion emissions

Emily A. Bruns[a]*, Jay G. Slowik[a], Imad El Haddad[a], Dogushan Kilic[a], Felix Klein[a], Josef Dommen[a], Brice Temime-Roussel[b], Nicolas Marchand[b], Urs Baltensperger[a] and André S. H. Prévôt[a]*

[a]*Laboratory of Atmospheric Chemistry, Paul Scherrer Institute, 5232 Villigen, Switzerland*

[b]*Aix Marseille Université, CNRS, LCE, Marseille, France*

[b]*Aix Marseille Université, CNRS, LCE UMR 7376, 13331, Marseille, France*

Correspondence to: E. A. Bruns (emily.bruns@psi.ch) or A. S. H. Prévôt (andre.prevot@psi.ch)

August 21, 2016

For submission to *Atmospheric Chemistry and Physics*

17 **Abstract**

18 Organic gases emitted during the flaming phase of residential wood combustion are

19 characterized individually and by functionality using proton transfer reaction time-of-flight mass

20 spectrometry. The evolution of the organic gases is monitored during photochemical aging.

21 Primary gaseous emissions are dominated by oxygenated species (e.g., acetic acid, acetaldehyde,

22 phenol and methanol), many of which have deleterious health effects and play an important role

23 in atmospheric processes such as secondary organic aerosol formation and ozone production.

24 Residential wood combustion emissions differ considerably from open biomass burning in both

25 absolute magnitude and relative composition. Ratios of acetonitrile, a potential biomass burning

26 marker, to CO are considerably lower (~0.09 pptv ppbv^{-1}) than those observed in air masses

27 influenced by open burning (~1-2 pptv ppbv^{-1}), which may make differentiation from

28 background levels difficult, even in regions heavily impacted by residential wood burning.

29 Considerable formic acid forms during aging (~200-600 mg kg^{-1} at an OH exposure of (4.5-

30 5.5)$\times 10^7$ molec cm^{-3} h), indicating residential wood combustion can be an important local source

31 for this acid, the quantities of which are currently underestimated in models. Phthalic anhydride,

32 a naphthalene oxidation product, is also formed in considerable quantities with aging (~55-75 mg

33 kg^{-1} at an OH exposure of (4.5-5.5)$\times 10^7$ molec cm^{-3} h). Although total NMOG emissions vary

34 by up to a factor of ~9 between burns, SOA formation potential does not scale with total NMOG

35 emissions and is similar in all experiments. This study is the first thorough characterization of

36 both primary and aged organic gases from residential wood combustion and provides a

37 benchmark for comparison of emissions generated under different burn parameters.

13

1 Introduction

Residential wood combustion is a source of gaseous and particulate emissions in the atmosphere, including a complex mixture of non-methane organic gases (NMOGs) (McDonald et al., 2000; Schauer et al., 2001; Hedberg et al., 2002; Jordan and Seen, 2005; Pettersson et al., 2011; Evtyugina et al., 2014; Reda et al., 2015). NMOGs impact climate (Stocker et al., 2013) and health (Pouli et al., 2003; Bølling et al., 2009) both directly and through the formation of products during atmospheric processing (Mason et al., 2001; Kroll and Seinfeld, 2008; Shao et al., 2009), which makes NMOG characterization critical. Although two studies have speciated a large fraction of the NMOG mass emitted during residential wood combustion in commercial burners (McDonald et al., 2000; Schauer et al., 2001), these studies relied on offline chromatographic approaches, which are time consuming in terms of sample preparation and analysis and can introduce both positive and negative artifacts (Nozière et al., 2015). Relatively recently, the proton transfer reaction mass spectrometer (PTR-MS) has emerged as a powerful tool for online quantification of atmospherically-relevant NMOGs (Lindinger et al., 1998; Jordan et al., 2009) eliminating many of the artifacts associated with offline approaches. NMOGs emitted during open burning of a variety of biomass fuels in the laboratory have been recently quantified using a high resolution proton transfer reaction time-of-flight mass spectrometer (PTR-ToF-MS) (Stockwell et al., 2015) and select nominal masses were followed during aging of residential wood combustion emissions using a quadrupole PTR-MS (Grieshop et al., 2009a). However, a complete high-resolution characterization of residential wood combustion emissions has yet to be performed.

The quantities and composition of NMOGs emitted during residential wood combustion are highly dependent on a number of parameters including wood type, appliance type and burn

14

61   conditions, and as few studies have characterized these NMOGs (McDonald et al., 2000; Schauer

62   et al., 2001; Hedberg et al., 2002; Jordan and Seen, 2005; Pettersson et al., 2011; Evtyugina et

63   al., 2014; Reda et al., 2015), further work is needed to constrain emission factors, as highlighted

64   in the recent review article by Nozière et al. (2015). Also, little is known about the evolution of

65   NMOGs from residential wood combustion with aging.

66   In this study, we present results from the first use of a smog chamber and a PTR-ToF-MS to

67   characterize primary and aged gaseous emissions from residential wood combustion in real-time.

68   This novel approach allows for an improved characterization of NMOG emissions, particularly

69   oxygenated NMOGs, which are a considerable fraction of the total NMOG mass emitted during

70   residential wood combustion (McDonald et al., 2000; Schauer et al., 2001). This study focuses

71   on a narrow set of burn conditions, namely the flaming phase of beech wood combustion, in

72   order to generate as reproducible emissions as possible for a complementary investigation of the

73   effects of parameters such as temperature on the emissions. While these experiments are a

74   narrow representation of real-world conditions, this novel work provides a benchmark and

75   direction for future wood combustion studies.

76   **2 Methods**

77   **2.1 Emission generation and smog chamber operation**

78   Beech (*Fagus sylvatica*) logs are combusted in a residential wood burner (Figure S1; single

79   combustion chamber, operated in single batch mode; Avant, 2009, Attika) and emissions are

80   sampled from the chimney through a heated line (473 K), diluted by a factor of ~8-10 using an

81   ejector diluter (473 K, DI-1000, Dekati Ltd.) and injected into the smog chamber (~7 m^3)

82   through a heated line (423 K). Emissions are sampled during the stable flaming phase of the

83 burn and modified combustion efficiencies (MCEs), defined as the ratio between CO_2 and the

84 sum of CO and CO_2, range from 0.974-0.978 (Table 1).

85 Emissions are injected for 11-21 min and total dilution factors range from ~100-200. All

86 experiments are conducted under similar conditions with starting wood masses in the burner of

87 2.9±0.3 kg and a wood moisture content of 19±2%. The smog chamber has an average

88 temperature of 287.0±0.1 K and a relative humidity of 55±3% over all five experiments.

89 Experimental parameters and primary emission values are summarized in Table S1. After

90 characterization of the primary emissions, as described below, a single dose of d9-butanol (2 µl,

91 butanol-D9, 98%, Cambridge Isotope Laboratories) is injected into the chamber and a continuous

92 injection of nitrous acid in air (2.3-2.6 l min^{-1}, ≥99.999%, Air Liquide) into the chamber begins.

93 The decay of d9-butanol measured throughout aging is used to estimate hydroxyl radical (OH)

94 exposures (Barmet et al., 2012). Nitrous acid produces OH upon irradiation in the chamber and

95 is used to increase the degree of aging. Levels of NO_x in the chamber prior to aging range from

96 ~165 0-350 ppbv and increases to ~250-380 ppbv after reaching OH exposures of ~(4.5-5.5)×10^7

97 molec cm^{-3} h (NO_x data unavailable for experiment 1). The small continuous dilution in the

98 chamber during aging due to the constant nitrous acid injection is accounted for using CO as an

99 inert tracer. The chamber contents are irradiated with UV light (40 lights, 90-100 W, Cleo

100 Performance, Philips) (Platt et al., 2013) for 4.5-6 h (maximum OH exposures of (4.7-6.8)×10^7

101 molec cm^{-3} h which corresponds to ~2-3 days of aging in the atmosphere at an OH concentration

102 of 1×10^6 molec cm^{-3}). Reported quantities of aged species are taken at OH exposures of (4.5-

103 5.5)×10^7 molec cm^{-3} h (Table 1; ~1.9-2.3 days of aging in the atmosphere at an OH

104 concentration of 1×10^6 molec cm^{-3}) (Barmet et al., 2012).

105 **2.2 Gas-phase analysis**

16

106   NMOGs with a proton affinity greater than that of water are measured using a PTR-ToF-MS

107   (PTR-ToF-MS 8000, Ionicon Analytik GmbH) and CO_2, CO and CH_4 are measured using cavity

108   ring-down spectroscopy (G2401, Picarro, Inc.). The PTR-ToF-MS operates with hydronium ion

109   ($[H_2O+H]^+$) as the reagent, a drift tube pressure of 2.2 mbar, a drift tube voltage of 543 V and a

110   drift tube temperature of 90°C leading to a ratio of the electric field (E) and the density of the

111   buffer gas (N) in the drift tube (reduced electric field, E/N) of 137 Townsend (Td). The

112   transmission function is determined using a gas standard of six NMOGs of known concentration

113   (methanol, acetaldehyde, propan-2-one, toluene, *p*-xylene, 1,3,5-trimethylbenzene; Carbagas).

114   As the RH and temperature of the sampled air is similar in all experiments, changes in the

115   detection efficiency of individual species are not expected.

116   PTR-ToF-MS data are analyzed using the Tofware post-processing software (version 2.4.5,

117   TOFWERK AG, Thun, Switzerland; PTR module as distributed by Ionicon Analytik GmbH),

118   running in the Igor Pro 6.3 environment (version 6.3, Wavemetrics Inc.). The minimum

119   detection limit is taken as three standard deviations above the background, where the standard

120   deviation is determined from the measurements of each ion in the chamber prior to emission

121   injection. Isotopic contributions are constrained during peak fitting and are accounted for in

122   reported concentrations. Possible molecular formulas increase with increasing *m/z*, making

123   accurate peak assignments difficult in the higher *m/z* range. Mass spectral data from *m/z* 33 to

124   *m/z* 130 are assigned molecular formulas, as well as the [18]O isotope of the reagent ion and signal

125   above *m/z* 130 corresponding to compounds previously identified during residential wood

126   combustion (McDonald et al., 2000; Schauer et al., 2001; Hedberg et al., 2002; Jordan and Seen,

127   2005; Pettersson et al., 2011; Evtyugina et al., 2014; Reda et al., 2015). All signal above *m/z* 130

128   is included in total NMOG mass quantification. Using this approach, ~94-97% of the total

129   NMOG mass measured using the PTR-ToF-MS has an ion assignment.

130   The reaction rate constant of each species with the reagent ion in the drift tube is needed to

131   convert raw signal to concentration. When available, individual reaction rate constants are

132   applied to ions assigned a structure (Cappellin et al., 2012) (Table S2~~1~~), otherwise a default

133   reaction rate constant of 2×10^{-9} cm^3 s^{-1} is applied. For possible isomers, the reaction rate

134   constant is taken as the average of available values. Approximately 60-70% of the total NMOG

135   mass is comprised of compounds with known rate constants. NMOG signal is normalized to

136    $[H_2^{18}O+H]^+$ to convert to concentration. Emission factors (EFs) normalize concentrations to the

137   total wood mass burned (e.g., mg kg^{-1} reads as mg of species emitted per kg wood burned) to

138   facilitate comparison between experiments and are calculated as described previously (Andreae

139   and Merlet, 2001; Bruns et al., 2015a).

140   PTR-ToF mass spectrometry is a relatively soft ionization technique generally resulting in

141   protonation of the parent NMOG ($[M+H]^+$), although some compounds are known to produce

142   other ions, for example through fragmentation or rearrangement (e.g., Baasandorj et al. (2015)).

143   Reactions potentially leading to considerable formation of species besides $[M+H]^+$ are discussed

144   in the Supplement. The extent to which reactions leading to ions other than $[M+H]^+$ occurs is

145   dependent on instrument parameters such as *E*/*N*. The unknown relative contributions of various

146   isomers makes it difficult to account for reactions generating ions besides $[M+H]^+$ and thus, no

147   fragmentation corrections are applied. Emission factors of compounds likely to undergo

148   extensive reaction to form products besides $[M+H]^+$ (i.e., methylcyclohexane (Midey et al.,

149   2003), ethyl acetate (Baasandorj et al., 2015) and saturated aliphatic aldehydes (Buhr et al.,

150   2002), with the exception of acetaldehyde) are not reported. Due to interferences, butenes

151   ($[C_4H_8+H]^+$) are not quantified.

152   **3 Results and Discussion**

153   **3.1 NMOG emissions**

154   In all experiments, the largest EFs for a single gas-phase species correspond to CO_2 (1770-1790

155   g kg^{-1}) and CO (27-30 g kg^{-1}) (Table 2), which are in good agreement with previous

156   measurements from residential beech logwood combustion where CO_2 EFs of ~1800 g kg^{-1} and

157   CO EFs of ~20-70 g kg^{-1} were measured (Ozil et al., 2009; Schmidl et al., 2011; Kistler et al.,

158   2012; Evtyugina et al., 2014; Reda et al., 2015). Methane is also emitted in considerable

159   quantities (1.5-2.8 g kg^{-1}), similar to previously observed values for beech wood burning in

160   fireplaces (0.5-1 g kg^{-1} (Ozil et al., 2009), however, at generally lower levels than total NMOGs

161   (1.5-13 g kg^{-1}). Total NMOG EFs from beech wood combustion have not been previously

162   reported, but values are similar to studies of residential wood stove burning of different

163   hardwoods which have attempted a detailed quantification of total NMOGs, such as McDonald

164   et al. (2000) (6.2-55.3 g kg^{-1} for a hardwood mixture) and Schauer et al. (2001) (6.7 g kg^{-1} for

165   oak). Total NMOG quantities reported in this study refer to species quantified using the PTR-

166   ToF-MS.

167   Although a large fraction of atmospherically-relevant organic gases are measured using the PTR-

168   ToF-MS, some species are not quantitatively detected, including those with a proton affinity less

169   than water (i.e., small alkanes). Based on previous studies of residential burning, alkanes are

170   estimated to contribute less than ~5% to the NMOG mass of either hard or softwood and the sum

171   of alkenes and alkynes, some of which are quantifiable with the PTR-ToF-MS, are estimated to

19

172   contribute less than ~15% to the total measured NMOG mass (McDonald et al., 2000; Schauer et

173   al., 2001).

174   Figure 1 shows the primary NMOG mass spectrum for each experiment classified by NMOG

175   functionality and the fractional contribution of NMOG functional groups to the total NMOG

176   mass. EFs for individual compounds are presented in Table 2. For ease of reading, nominal *m/z*s

177   are presented in the text and figures, however, monoisotopic *m/z*s for all identified species can be

178   found in Tables 2 and S32. Separation of isobaric species is possible using the PTR-ToF-MS,

179   however, isomers remain indistinguishable. Quantities of gas-phase species generated during

180   residential wood combustion depend on a variety of parameters, such as type of burner and wood

181   species. However, many compounds are commonly emitted and structures are assigned to

182   observed ions based on previously identified species (McDonald et al., 2000; Schauer et al.,

183   2001; Hedberg et al., 2002; Jordan and Seen, 2005; Pettersson et al., 2011; Evtyugina et al.,

184   2014; Reda et al., 2015). A few small, unambiguous ions are also assigned a structure, including

185   methanol, formic acid and acetonitrile. Approximately 70% of the total NMOG mass measured

186   using the PTR-ToF-MS is assigned a structure based on this method.

187   NMOGs are categorized by functional groups including: oxygenated, total C_xH_y, nitrogen-

188   containing and other. Oxygenated subcategories include: acids (comprised of non-aromatic

189   acids), carbonyls (comprised of non-aromatic carbonyls), oxygenated aromatics (not including

190   furans), furans, O-containing (comprised of structurally unassigned oxygenated compounds and

191   multifunctional oxygenated compounds) and O- and N-containing (comprised of species

192   containing both oxygen and nitrogen atoms). Species categorized as N-containing contain no

193   oxygen atoms. Total C_xH_y subcategories include: aromatic hydrocarbons, and non-aromatic and

194   structurally unassigned species (referred to as C_xH_y in the text and figures). Higher molecular

195   weight species lacking an ion assignment are categorized as "other". In the case of possible

196   isomers, ions are categorized according to the species most likely to dominate based on previous

197   studies (McDonald et al., 2000; Schauer et al., 2001; Hedberg et al., 2002; Jordan and Seen,

198   2005; Pettersson et al., 2011; Evtyugina et al., 2014; Reda et al., 2015).

199   Oxygenated species contribute ~68-94% to the total primary NMOG mass, which has important

200   atmospheric implications due to the role of these compounds in photochemical reactions, for

201   example by altering O_3 and peroxide formation (Mason et al., 2001; Shao et al., 2009).

202   McDonald et al. (2000) and Schauer et al. (2001) previously observed the dominance of

203   oxygenated NMOGs during residential burning of other wood types, whereas Evtyugina et al.

204   (2014) found that benzene and benzene derivatives contributed 59% to the total measured

205   NMOGs, compared to only 26% from oxygenated compounds for residential burning of beech

206   wood in a woodstove. However, Evtyugina et al. (2014), as well as McDonald et al. (2000) and

207   Schauer et al. (2001), did not include emissions from all lower molecular weight NMOGs, such

208   as acetic acid. Oxygenated NMOGs are also reported as a large fraction of NMOGs emitted

209   during open burning of many biomass fuels (Gilman et al., 2015; Stockwell et al., 2015).

210   Acids are the most abundant subclass of species in all experiments with an average EF of

211   2000±2000 mg kg^{-1} and acetic acid ($[C_2H_4O_2+H]^+$ at nominal m/z 61) is the most highly emitted

212   compound in all experiments. In addition to acetic acid, $[C_2H_4O_2+H]^+$ can correspond to

213   glycolaldehyde, however, Stockwell et al. (2015) found that acetic acid contributes ~75-93% to

214   $[C_2H_4O_2+H]^+$ during open burning of black spruce (*Picea mariana)* and ponderosa pine (*Pinus*

215   *ponderosa*) and thus, it is expected that this ion is also largely attributable to acetic acid in the

216   current study. Acetic acid and formic acid ($[CH_2O_2+H]^+$ at nominal m/z 47) are the most

217   abundant carboxylic acids in the atmosphere and are important contributors to atmospheric

218   acidity (Chebbi and Carlier, 1996). However, the sources of these acids are poorly understood

219   (Paulot et al., 2011) and data on their EFs from residential wood combustion are relatively

220   unknown. The high acetic acid EFs found here indicate that residential wood combustion can be

221   an important local source of this acid. Interestingly, the enhancement of acetic acid ($\Delta C_2H_4O_2$)

222   over background levels relative to CO enhancement (ΔCO) in the current study ranges from ~6

223   to 80 pptv ppbv^{-1} (Table 1), which is much higher than the average 0.58 pptv ppbv^{-1} (sum of gas

224   and aerosol phase) measured in an Alpine valley heavily impacted by residential wood

225   combustion in winter (Gaeggeler et al., 2008). Further work is needed to investigate the source

226   of this discrepancy, as limited ambient measurements are available from regions heavily

227   impacted by residential wood combustion. However, it is possible that the ambient

228   measurements were dominated by emissions produced during poor burning conditions (e.g.,

229   starting phase) where CO EFs are expected to be higher than during the stable burning phase

230   investigated in the current study.

231   The sum of oxygenated and non-oxygenated aromatic compounds contribute ~7-30% (800±300

232   mg kg^{-1}) to the total primary NMOG mass with benzene ($[C_6H_6+H]^+$ at nominal m/z 79), phenol

233   ($[C_6H_6O+H]^+$ at nominal m/z 95), and naphthalene ($[C_{10}H_8+H]^+$ at nominal m/z 129) as the three

234   most dominant species. Oxidation products of aromatic species are the largest contributors to

235   residential wood combustion SOA in this study (Bruns et al., 2016) and both aromatic and

236   related oxidation products are of interest due to their particularly deleterious effects on health (Fu

237   et al., 2012).

238   For the other functional group categories, carbonyl and alcohols contribute ~8-12% (600±600

239   mg kg^{-1}) and ~3-5% (300±300 mg kg^{-1}), respectively, to the total NMOG mass. In general, the

240   most highly emitted carbonyl compound is acetaldehyde ($[C_2H_4O+H]^+$ at nominal m/z 45).

241 Methanol ($[CH_3OH+H]^+$ at nominal m/z 33) is the most highly emitted alcohol, although other

242 acyclic alcohols can undergo extensive fragmentation in the mass spectrometer. Furans are only

243 a minor contributor to the total primary NMOG mass, contributing ~3-5% (300 ± 300 mg kg^{-1}),

244 but are of potential interest as several furans were recently identified as SOA precursors (Gómez

245 Alvarez et al., 2009) and possible open biomass burning markers (Gilman et al., 2015).

3.2 Burn variability

247 Although the same compounds are emitted during all burns, there is variability in EFs between

248 experiments despite efforts to replicate burns as closely as possible and the fact that the MCE for

249 each experiment falls within a narrow range (0.974-0.978) (Table 1). Experiments 2 and 3 show

250 marked differences in total NMOG EFs and NMOG composition compared to experiments 1, 4

251 and 5. For example, the total NMOG EF is ~9 times higher in experiment 2 compared to

252 experiment 5 (Table 2). Acetic acid EFs vary by a factor of ~15 between burns, with high

253 emissions in experiments 2 and 3 relative to experiments 1, 4 and 5. The total emission of

254 oxygenated species also correlates with acetic acid emissions, with total oxygenated EFs

255 considerably higher in experiments 2 and 3 than in experiments 1, 4 and 5. In contrast, aromatic

256 hydrocarbons and C_xH_y EFs show no correlation with total oxygenated species or acetic acid

257 EFs. Interestingly, differences in black carbon EFs, primary organic aerosol EFs and primary

258 organic aerosol mass to black carbon ratios are also not observed between these two groupings of

259 experiments (2, 3 and 1, 4, 5), as presented previously (Bruns et al., 2016). Enhancements in the

260 average EF for the different functional groups in experiments 2 and 3 relative to experiments 1, 4

261 and 5 are shown in Figure 2.

262 The differences in EFs due to inter-burn variability illustrate the difficulty in constraining EFs

263 from residential wood combustion. The burner is housed in an uninsulated building and the

264 emission profile variability could be due to effects of outdoor temperature variability on the

265 burner. For example, emission profiles from burning lignite and pyrolysis of bark and other

266 biomass sources have been shown to vary with burn temperature (Hansson et al., 2004; Šyc et

267 al., 2011). Further work to constrain the possible range of EFs generated under different

268 conditions is critical for improving model inputs. EFs are also dependent on factors such as

269 appliance type and fuel loading and further work is needed to characterize the emissions and the

270 evolution of these emissions with aging generated from burning of different wood types and

271 under different burn parameters.

272 **3.3 Biomass burning tracers**

273 Individual compounds emitted exclusively or in large quantities during biomass burning are of

274 interest for source apportionment and compounds contributing to SOA formation are of

275 particular interest for climate and health (Figure 3). Acetonitrile is used as an ambient gas-phase

276 marker for open biomass burning (de Gouw et al., 2003; Singh et al., 2003). In the current

277 experiments, acetonitrile EFs are relatively low (3.5 ± 0.3 mg kg^{-1}) compared to open biomass

278 burning (~20-1000 mg kg^{-1}) (Yokelson et al., 2008; Yokelson et al., 2009; Akagi et al., 2013;

279 Stockwell et al., 2015), likely due to different burn conditions (e.g., oxygen availability). The

280 enhancements of acetonitrile over background levels relative to CO enhancement,

281 $\Delta CH_3CN/\Delta CO$, are ~0.08-0.1 pptv ppbv^{-1} (Table 1). This is slightly lower than the only

282 previously published residential wood combustion measurements (0.1 to 0.8 pptv ppbv^{-1})

283 (Grieshop et al., 2009a), but is much lower than $\Delta CH_3CN/\Delta CO$ measurements in ambient air

284 masses impacted by open biomass burning (~1-2 pptv ppbv^{-1}) (Holzinger et al., 1999; Andreae

285   and Merlet, 2001; Christian et al., 2003; de Gouw et al., 2003; Jost et al., 2003; Holzinger et al.,

286   2005; de Gouw et al., 2006; Warneke et al., 2006; Yokelson et al., 2008; de Gouw et al., 2009;

287   Yokelson et al., 2009; Aiken et al., 2010; Akagi et al., 2013). However, $\Delta CH_3CN/\Delta CO$ during

288   open burning has been shown to depend strongly on fuel type; Stockwell et al. (2015) observed

289    $\Delta CH_3CN/\Delta CO$ values from 0.0060-7.1 pptv ppbv^{-1} for individual open burns of different

290   biomass types in the laboratory. In agreement with the current study, ambient measurements of

291   acetonitrile made in Colorado (USA) were not associated with fresh residential burning

292   emissions (Coggon et al., 2016). Lower ambient measurements of nitrogen-containing NMOGs

293   (including acetonitrile) during residential burning compared to open burning were attributed to

294   the generally lower nitrogen content in fuels burned residentially (Coggon et al., 2016). Lower

295   nitrogen content of the fuel is likely a contributor to the relatively low acetonitrile emissions in

296   the current study.

297   The primary emission factors of other nitrogenated species, such as C_3H_3N (likely corresponding

298   to acrylonitrile) and HNCO ranged in our study from 3.6-6.4 mg kg^{-1} and BDL-11 mg kg^{-1},

299   respectively. Emission factors of C_3H_3N in the current study are lower than those observed

300   during open burning (e.g., ~10-90 mg kg^{-1} (Akagi et al., 2013)), as expected based on the lower

301   acetonitrile emission factors observed in the current study and the findings of Coggon et al.

302   (2016)."

303   –Further work is needed to investigate CH_3CN emissions from residential burning of other wood

304   types, as well as emissions during other burning phase (e.g., smoldering). However, these low

305   enhancements may be difficult to differentiate from ambient background levels, making

306   acetonitrile a poor marker for residential wood combustion under these burning conditions.

307 Coggon et al. (2016) concluded that acetonitrile may not be a good tracer for residential burning

308 in urban areas.

309 The interference from isobaric compounds when quantifying acetonitrile using a PTR-MS is an

310 important consideration when high resolution data are not available. Previously, several studies

311 have determined this interference is minimal during open biomass burning (de Gouw et al., 2003;

312 Warneke et al., 2003; Christian et al., 2004; Warneke et al., 2011). Recently, Dunne et al. (2012)

313 quantified interferences with acetonitrile measurements in polluted urban air using a quadrupole

314 PTR-MS and found contributions of 5-41% to m/z 42 from non-acetonitrile ions including:

315 $[C_3H_6]^+$ and the ^{13}C isotope contribution from $[C_3H_5]^+$. In the current study, in addition to

316 contributions from $[C_3H_6]^+$ and the isotopic contribution from $[C_3H_5]^+$, ~30-50% of the total

317 signal at m/z 42 is due to $[C_2H_2O]^+$, which is presumably a fragment from higher molecular

318 weight species. The total contribution to m/z 42 from species besides acetonitrile is ~70-85%.

319 Although an investigation into the effects of the PTR-MS operating conditions (e.g., $[O_2]^+$ signal

320 from ion source, E/N affecting fragmentation) is outside the scope of the current study, the

321 possibility of considerable non-acetonitrile signal at m/z 42 should be taken into consideration

322 when using nominal mass PTR-MS data to quantify acetonitrile from residential wood

323 combustion.

324 Methanol is also used to identify air masses influenced by open biomass burning and

325 enhancement over background levels relative to CO enhancement ($\Delta CH_3OH/\Delta CO$) is typically

326 ~1-80 pptv ppbv^{-1} in ambient and laboratory measurements of fresh open biomass burning

327 emissions (Holzinger et al., 1999; Goode et al., 2000; Andreae and Merlet, 2001; Christian et al.,

328 2003; Yokelson et al., 2003; Singh et al., 2004; Tabazadeh et al., 2004; Holzinger et al., 2005; de

329 Gouw et al., 2006; Gaeggeler et al., 2008; Yokelson et al., 2008; Yokelson et al., 2009; Akagi et

330 al., 2013; Stockwell et al., 2015; Müller et al., 2016). Here, we find similar values ranging from

331 ~2-20 pptv ppbv^{-1} (Table 1), in agreement with Gaeggeler et al. (2008) who measured a

332 $\Delta CH_3OH/\Delta CO$ value of 2.16 pptv ppbv^{-1} in an Alpine valley heavily impacted by residential

333 wood combustion emissions in winter.

3.4 Chamber studies of NMOG aging

335 Previous investigations of aged residential wood combustion emissions have largely focused on

336 the evolution of the aerosol phase (Grieshop et al., 2009a; Grieshop et al., 2009b; Hennigan et

337 al., 2010; Heringa et al., 2011; Bruns et al., 2015a; Bruns et al., 2015b; Bruns et al., 2016) and

338 little is known about the evolution of the gas phase. The evolution of the NMOG functional

339 group categories with increasing OH exposure is shown in Figure 4. Figure 5 shows the absolute

340 change in mass spectral signal between the aged and primary NMOG quantities. Although an

341 increase in NMOG mass could be expected with aging due to oxygenation, total NMOG mass

342 decreases by ~5-30% at an OH exposure of $(4.6-5.5)\times10^7$ molec cm^{-3} h relative to the primary

343 emissions in experiments 1-4, likely due to the conversion of species from the gas to particle

344 phase, the mass of which increased considerably with aging (Bruns et al., 2016), and the

345 formation of gas-phase species not quantified here (e.g., formaldehyde). Previous investigation

346 of these experiments determined that the conversion of NMOGs traditionally included in models

347 to SOA accounts for only ~3-27% of the observed SOA, whereas ~84-116% of the SOA is

348 explained by inclusion of non-traditional precursors, including naphthalene and phenol (Bruns et

349 al., 2016). The total NMOG mass increases slightly, by ~5%, in experiment 5. Quantities of

350 individual NMOGs and NMOG functional group categories after reaching an OH exposure of

351 $(4.6-5.5)\times10^7$ molec cm^{-3} h are presented in Table S3. In addition to gas to particle phase

352 partitioning and formation of gas-phase species not quantified here, a decrease in NMOG mass

with aging could also be due to losses of gas-phase species to the chamber walls (Zhang et al., 2014; Bian et al., 2015). Measurements of NMOGs in the chamber prior to aging are stable, indicating that the chamber walls are not a sink for NMOGs, but rather that NMOGs are in equilibrium with the chamber walls, particles and the gas phase. Zhang et al. (2014) show that the rate of NMOG wall loss is proportional to seed aerosol concertation and OH concentration, both of which were relatively high in the current experiments (Table S1; OH concentrations were ~1.4x10^7 molec cm^{-3}). Under these experimental conditions, NMOG wall losses are not expected to be large. Future studies are needed to investigate vapor wall loss of residential wood combustion emissions during aging.

Subcategories of oxygenated species behave differently with aging. For example, total quantities (mg kg^{-1}) of oxygenated aromatic species decrease by factors of ~7-15 and furan quantities decrease by factors of ~4-9, whereas all other oxygenated subcategories, as well as N-containing species, remain within a factor of 2 of primary values at an OH exposure of (4.6-5.5)×10^7 molec cm^{-3} h. Aromatic hydrocarbons and C_xH_y quantities decrease with aging by factors of ~1.5-3. The large decreases in oxygenated aromatic species and furans illustrate the highly reactive nature of these species with respect to OH. The evolution of the bulk NMOG elemental composition during aging is shown in Figure S2 in the Supplement.

In all experiments, formic acid quantities increases considerably with aging (by factors of ~5-50), as does $[C_4H_2O_3+H]^+$ at nominal m/z 99 (by factors of ~2-3), which likely corresponds to maleic anhydride, both of which are formed during the oxidation of aromatic species among other compounds (Bandow et al., 1985; Sato et al., 2007; Praplan et al., 2014). However, the fragment resulting from the loss of water from maleic acid cannot be distinguished from maleic anhydride using the PTR-ToF-MS. Formic acid is underestimated in models, likely due to

376 missing secondary sources (Paulot et al., 2011) and these results indicate that aging of residential

377 wood combustion emissions can result in considerable secondary formic acid production. The

378 signal at m/z 149, corresponding to $[C_8H_4O_3+H]^+$, increases by factors of ~2-7 with aging. This

379 ion likely corresponds to phthalic anhydride, which is a known naphthalene oxidation product

380 (Chan et al., 2009).

381 Acetic acid formation has been observed in some ambient, open biomass burning plumes with

382 aging (Goode et al., 2000; Hobbs et al., 2003; Yokelson et al., 2003), whereas not in others (de

383 Gouw et al., 2006) and a doubling of m/z 61, likely dominated by acetic acid, was observed

384 during aging of residential burning emissions in a previous laboratory study (Grieshop et al.,

385 2009a). In the current study, no increase in the average acetic acid concentration relative to

386 $CO_{(g)}$ is observed (Table 1). Note that this implies production of secondary acetic acid that

387 compensates for the expected consumption of ~8-10% of primary acetic acid by reaction with

388 OH at an OH exposure of $(4.5-5.5)\times10^7$ molec cm^{-3} h. These results indicate that acetic acid

389 from residential burning of beech wood is dominated by primary emissions of this species (Table

390 1). As with acetic acid, there are discrepancies in methanol behavior as open biomass burning

391 plumes undergo aging (Goode et al., 2000; Yokelson et al., 2003; Tabazadeh et al., 2004;

392 Holzinger et al., 2005; de Gouw et al., 2006; Akagi et al., 2013). As described by Akagi et al.

393 (2013), methanol enhancement has been hypothesized to correlate with terpene concentration

394 and here, methanol remains within ~1-20% of the primary value after exposure to $(4.5-5.5)\times10^7$

395 molec cm^{-3} h OH (Table 1), which is expected based on the reaction with OH (Overend and

396 Paraskevopoulos, 1978) and the low terpene concentrations. Monoterpene concentrations are

397 below the detection limit in all experiments and isoprene emissions are relatively low (Table 2).

29

398 We have previously identified the compounds contributing to the majority of the SOA formed

399 during these experiments (Bruns et al., 2016). The average EF for each of these species is shown

400 in Figure 3. Figure S32 shows the observed decay of the largest SOA precursors contributing the

401 most to SOA formation during aging in the chamber compared to the expected decay based on

402 the OH concentration in the chamber and the reaction rate with respect to OH. There is generally

403 good agreement between the observed and calculated decay for each compound which supports

404 the structural assignment of each ion. For 2-methoxyphenol and 2,6-dimethoxyphenol (Figure

405 S3 f and i, respectively), the agreement between the observed and calculated decays is not as

406 good as for the other compounds, with slower decays than predicted. This discrepancy may be

407 due to fragmentation of related compounds to form 2-methoxyphenol and 2,6-dimethoxyphenol

408 in the instrument or formation of these compounds in the chamber during oxidation. For o-

409 benzenediol, the decays are initially faster than expected and then become slower with increased

410 aging, possibly due to the presence of isomers with different reaction rates with respect to OH.

411 **3.5 Aged emission variability**

412 As described above, the overall primary emission profiles, as well as total NMOG

413 emissionsmass emitted, vary considerably for experiments 2 and 3 compared to experiments 1, 4

414 and 5, with considerably much higher total NMOG emissions in experiments 2 and 3. It is

415 expected that the aged emission profiles also exhibit variability based on the primary emissions.

416 Total acid and O-containing species decrease with aging in experiments 2 and 3, in contrast to

417 experiments 1, 4 and 5, where these classes increase with aging (Figure 4). Formic acid shows

418 the largest increase with aging in all experiments (~190-480 mg kg^{-1} relative to the primary EF,

419 Figure 5), however, in experiments 1, 4 and 5, this increase contributes much more to the total

420 acid mass as the total acid mass is ~5-15 times lower compared to experiments 2 and 3. An

30

analogous case occurs for maleic anhydride for the O-containing class of compounds. As formic acid and maleic anhydride are formed from the oxidation of aromatic compounds (Bandow et al., 1985; Sato et al., 2007; Praplan et al., 2014), among others, a higher fraction of aromatic species to the total NMOG emissions will contribute to increases in acid and O-containing NMOGs. Inclusion of NMOGs not quantified by PTR-ToF-MS could impact the trends observed in Figure 4.

To determine the impact of the high NMOG emission experiments (2 and 3) compared to the lower NMOG emission experiments (1, 4 and 5) on SOA formation potential, individual SOA precursors with published SOA yields are investigated. (Figure 3). The SOA formation potential for each of these 18 compounds is determined as the product of the primary EF and the best estimate SOA yield determined from the literature, as determined previously (Bruns et al., 2016). The total SOA formation potential for each experiment is taken as the sum of the individual SOA formation potentials. Interestingly, the SOA formation potential is similar in all experiments and the average enhancement of SOA formation potential in experiments 2 and 3 compared to the average of experiments 1, 4 and 5 is insignificant (Figure 2), despite the considerably different total NMOG EFs.

4 Conclusions

This study is the first detailed characterization of primary NMOGs from residential wood combustion using a PTR-ToF-MS and the first investigation of the evolution of the majority of these NMOGs with aging. Differences in EFs and profiles between residential burning and open burning can be considerable and these results illustrate the importance of considering these emission sources individually. While total emissions from open burning are much larger than

31

443 from residential burning, the societal relevance of residential wood burning emissions is

444 nontrivial. A large fraction of open biomass burning derives from wildfires in sparsely

445 populated regions (Ito and Penner, 2004), whereas residential wood combustion has been shown

446 to be a major fraction of wintertime submicron organic aerosol in densely populated

447 communities (Glasius et al., 2006; Krecl et al., 2008; Gonçalves et al., 2012; Guofeng et al.,

448 2012; Crippa et al., 2013; Herich et al., 2014; Tao et al., 2014; Paraskevopoulou et al., 2015).

449 Interestingly, MCE does not completely capture inter-burn variability, which is driven by

450 differences in oxygenated content. This work clearly shows that measurements of total NMOGs

451 or total hydrocarbon measurements are insufficient for estimating SOA formation potential from

452 residential wood combustion. While this work characterizes the stable burning of beech wood in

453 a modern woodstove, the composition and quantities of wood combustion emissions are highly

454 dependent on many factors and further work is needed to characterize the emissions and the

455 evolution of these emissions with aging generated from burning of different wood types and

456 under different burn parameters.

457 **Acknowledgements**

464 **References**

465 Aiken, A.C., de Foy, B., Wiedinmyer, C., DeCarlo, P.F., Ulbrich, I.M., Wehrli, M.N., Szidat, S.,
466 Prevot, A.S.H., Noda, J., Wacker, L., Volkamer, R., Fortner, E., Wang, J., Laskin, A.,
467 Shutthanandan, V., Zheng, J., Zhang, R., Paredes-Miranda, G., Arnott, W.P., Molina, L.T., Sosa,
468 G., Querol, X. and Jimenez, J.L.: Mexico city aerosol analysis during MILAGRO using high
469 resolution aerosol mass spectrometry at the urban supersite (T0) – Part 2: Analysis of the
470 biomass burning contribution and the non-fossil carbon fraction, Atmos. Chem. Phys. 10, 5315-
471 5341, 2010.

472
473 Akagi, S.K., Yokelson, R.J., Burling, I.R., Meinardi, S., Simpson, I., Blake, D.R., McMeeking,
474 G.R., Sullivan, A., Lee, T., Kreidenweis, S., Urbanski, S., Reardon, J., Griffith, D.W.T.,
475 Johnson, T.J. and Weise, D.R.: Measurements of reactive trace gases and variable O_3 formation
476 rates in some South Carolina biomass burning plumes, Atmos. Chem. Phys. 13, 1141-1165,
477 2013.

478
479 Andreae, M.O. and Merlet, P.: Emission of trace gases and aerosols from biomass burning,
480 Global Biogeochem. Cy. 15, 955-966, 2001.

481
482 Baasandorj, M., Millet, D.B., Hu, L., Mitroo, D. and Williams, B.J.: Measuring acetic and formic
483 acid by proton-transfer-reaction mass spectrometry: sensitivity, humidity dependence, and
484 quantifying interferences, Atmos. Meas. Tech. 8, 1303-1321, 2015.

485
486 Bandow, H., Washida, N. and Akimoto, H.: Ring-cleavage reactions of aromatic hydrocarbons
487 studied by FT-IR spectroscopy. I. Photooxidation of toluene and benzene in the NO_x-Air System,
488 B. Chem. Soc. Jpn. 58, 2531-2540, 1985.

489
490 Barmet, P., Dommen, J., DeCarlo, P.F., Tritscher, T., Praplan, A.P., Platt, S.M., Prévôt, A.S.H.,
491 Donahue, N.M. and Baltensperger, U.: OH clock determination by proton transfer reaction mass
492 spectrometry at an environmental chamber, Atmos. Meas. Tech. 5, 647-656, 2012.

493
494 Bian, Q., May, A.A., Kreidenweis, S.M. and Pierce, J.R.: Investigation of particle and vapor
495 wall-loss effects on controlled wood-smoke smog-chamber experiments, Atmos. Chem. Phys.
496 15, 11027-11045, 2015.

497
498 Bølling, A.K., Pagels, J., Yttri, K.E., Barregard, L., Sallsten, G., Schwarze, P.E. and Boman, C.:
499 Health effects of residential wood smoke particles: the importance of combustion conditions and
500 physicochemical particle properties, Part. Fibre Toxicol. 6, doi:10.1186/1743-8977-1186-1129,
501 2009.

502
503 Bruns, E.A., Krapf, M., Orasche, J., Huang, Y., Zimmermann, R., Drinovec, L., Močnik, G., El
504 Haddad, I., Slowik, J.G., Dommen, J., Baltensperger, U. and Prévôt, A.S.H.: Characterization of

505 primary and secondary wood combustion products generated under different burner loads,
506 Atmos. Chem. Phys. 15, 2825-2841, 2015a.

507
508 Bruns, E.A., El Haddad, I., Keller, A., Klein, F., Kumar, N.K., Pieber, S.M., Corbin, J.C.,
509 Slowik, J.G., Brune, W.H., Baltensperger, U. and Prévôt, A.S.H.: Inter-comparison of laboratory
510 smog chamber and flow reactor systems on organic aerosol yield and composition, Atmos. Meas.
511 Tech. 8, 2315-2332, 2015b.

512
513 Bruns, E.A., El Haddad, I., Slowik, J.G., Kilic, D., Klein, F., Baltensperger, U. and Prévôt,
514 A.S.H.: Identification of significant precursor gases of secondary organic aerosols from
515 residential wood combustion, Sci. Rep. 6, doi: 10.1038/srep27881, 2016.

516
517 Buhr, K., van Ruth, S. and Delahunty, C.: Analysis of volatile flavour compounds by Proton
518 Transfer Reaction-Mass Spectrometry: fragmentation patterns and discrimination between
519 isobaric and isomeric compounds, Int. J. Mass. Spectrom. 221, 1-7, 2002.

520
521 Cappellin, L., Karl, T., Probst, M., Ismailova, O., Winkler, P.M., Soukoulis, C., Aprea, E., Märk,
522 T.D., Gasperi, F. and Biasioli, F.: On quantitative determination of volatile organic compound
523 concentrations using proton transfer reaction time-of-flight mass spectrometry, Environ. Sci.
524 Technol. 46, 2283-2290, 2012.

525
526 Chan, A.W.H., Kautzman, K.E., Chhabra, P.S., Surratt, J.D., Chan, M.N., Crounse, J.D., Kürten,
527 A., Wennberg, P.O., Flagan, R.C. and Seinfeld, J.H.: Secondary organic aerosol formation from
528 photooxidation of naphthalene and alkylnaphthalenes: implications for oxidation of intermediate
529 volatility organic compounds (IVOCs), Atmos. Chem. Phys. 9, 3049-3060, 2009.

530
531 Chebbi, A. and Carlier, P.: Carboxylic acids in the troposphere, occurrence, sources, and sinks:
532 A review, Atmos. Environ. 30, 4233-4249, 1996.

533
534 Christian, T.J., Kleiss, B., Yokelson, R.J., Holzinger, R., Crutzen, P.J., Hao, W.M., Saharjo, B.H.
535 and Ward, D.E.: Comprehensive laboratory measurements of biomass-burning emissions: 1.
536 Emissions from Indonesian, African, and other fuels, J. Geophys. Res.-Atmos. 108,
537 doi:10.1029/2003JD003704, 2003.

538
539 Christian, T.J., Kleiss, B., Yokelson, R.J., Holzinger, R., Crutzen, P.J., Hao, W.M., Shirai, T. and
540 Blake, D.R.: Comprehensive laboratory measurements of biomass-burning emissions: 2. First
541 intercomparison of open-path FTIR, PTR-MS, and GC-MS/FID/ECD, J. Geophys. Res.-Atmos.
542 109, doi:10.1029/2003JD003874, 2004.

543

544 Coggon, M.M., Veres, P.R., Yuan, B., Koss, A., Warneke, C., Gilman, J.B., Lerner, B.M.,
545 Peischl, J., Aikin, K.C., Stockwell, C.E., Hatch, L.E., Ryerson, T.B., Roberts, J.M., Yokelson,
546 R.J. and de Gouw, J.A.: Emissions of nitrogen-containing organic compounds from the burning
547 of herbaceous and arboraceous biomass: Fuel composition dependence and the variability of
548 commonly used nitrile tracers, Geophys. Res. Lett. 43, 9903-9912, 2016.

549
550 Crippa, M., DeCarlo, P.F., Slowik, J.G., Mohr, C., Heringa, M.F., Chirico, R., Poulain, L.,
551 Freutel, F., Sciare, J., Cozic, J., Di Marco, C.F., Elsasser, M., Nicolas, J.B., Marchand, N., Abidi,
552 E., Wiedensohler, A., Drewnick, F., Schneider, J., Borrmann, S., Nemitz, E., Zimmermann, R.,
553 Jaffrezo, J.L., Prévôt, A.S.H. and Baltensperger, U.: Wintertime aerosol chemical composition
554 and source apportionment of the organic fraction in the metropolitan area of Paris, Atmos. Chem.
555 Phys. 13, 961-981, 2013.

556
557 de Gouw, J.A., Warneke, C., Parrish, D.D., Holloway, J.S., Trainer, M. and Fehsenfeld, F.C.:
558 Emission sources and ocean uptake of acetonitrile (CH_3CN) in the atmosphere, J. Geophys. Res.-
559 Atmos. 108, doi:10.1029/2002JD002897, 2003.

560
561 de Gouw, J.A., Warneke, C., Stohl, A., Wollny, A.G., Brock, C.A., Cooper, O.R., Holloway,
562 J.S., Trainer, M., Fehsenfeld, F.C., Atlas, E.L., Donnelly, S.G., Stroud, V. and Lueb, A.: Volatile
563 organic compounds composition of merged and aged forest fire plumes from Alaska and western
564 Canada, J. Geophys. Res.-Atmos. 111, doi:10.1029/2005JD006175, 2006.

565
566 de Gouw, J.A., Welsh-Bon, D., Warneke, C., Kuster, W.C., Alexander, L., Baker, A.K.,
567 Beyersdorf, A.J., Blake, D.R., Canagaratna, M., Celada, A.T., Huey, L.G., Junkermann, W.,
568 Onasch, T.B., Salcido, A., Sjostedt, S.J., Sullivan, A.P., Tanner, D.J., Vargas, O., Weber, R.J.,
569 Worsnop, D.R., Yu, X.Y. and Zaveri, R.: Emission and chemistry of organic carbon in the gas
570 and aerosol phase at a sub-urban site near Mexico City in March 2006 during the MILAGRO
571 study, Atmos. Chem. Phys. 9, 3425-3442, 2009.

572
573 Dunne, E., Galbally, I.E., Lawson, S. and Patti, A.: Interference in the PTR-MS measurement of
574 acetonitrile at *m/z* 42 in polluted urban air—A study using switchable reagent ion PTR-MS, Int.
575 J. Mass. Spectrom. 319–320, 40-47, 2012.

576
577 Evtyugina, M., Alves, C., Calvo, A., Nunes, T., Tarelho, L., Duarte, M., Prozil, S.O., Evtuguin,
578 D.V. and Pio, C.: VOC emissions from residential combustion of Southern and mid-European
579 woods, Atmos. Environ. 83, 90-98, 2014.

580
581 Fu, P.P., Xia, Q., Sun, X. and Yu, H.: Phototoxicity and environmental transformation of
582 polycyclic aromatic hydrocarbons (PAHs)—light-induced reactive oxygen species, lipid
583 peroxidation, and DNA damage, J. Environ. Sci. Heal. C 30, 1-41, 2012.

584

585 Gaeggeler, K., Prevot, A.S.H., Dommen, J., Legreid, G., Reimann, S. and Baltensperger, U.:
586 Residential wood burning in an Alpine valley as a source for oxygenated volatile organic
587 compounds, hydrocarbons and organic acids, Atmos. Environ. 42, 8278-8287, 2008.

588
589 Gilman, J.B., Lerner, B.M., Kuster, W.C., Goldan, P.D., Warneke, C., Veres, P.R., Roberts, J.M.,
590 de Gouw, J.A., Burling, I.R. and Yokelson, R.J.: Biomass burning emissions and potential air
591 quality impacts of volatile organic compounds and other trace gases from fuels common in the
592 United States, Atmos. Chem. Phys. 15, 13915-13938, 2015.

593
594 Glasius, M., Ketzel, M., Wåhlin, P., Jensen, B., Mønster, J., Berkowicz, R. and Palmgren, F.:
595 Impact of wood combustion on particle levels in a residential area in Denmark, Atmos. Environ.
596 40, 7115-7124, 2006.

597
598 Gómez Alvarez, E., Borrás, E., Viidanoja, J. and Hjorth, J.: Unsaturated dicarbonyl products
599 from the OH-initiated photo-oxidation of furan, 2-methylfuran and 3-methylfuran, Atmos.
600 Environ. 43, 1603-1612, 2009.

601
602 Gonçalves, C., Alves, C. and Pio, C.: Inventory of fine particulate organic compound emissions
603 from residential wood combustion in Portugal, Atmos. Environ. 50, 297-306, 2012.

604
605 Goode, J.G., Yokelson, R.J., Ward, D.E., Susott, R.A., Babbitt, R.E., Davies, M.A. and Hao,
606 W.M.: Measurements of excess O_3, CO_2, CO, CH_4, C_2H_4, C_2H_2, HCN, NO, NH_3, HCOOH,
607 CH_3COOH, HCHO, and CH_3OH in 1997 Alaskan biomass burning plumes by airborne Fourier
608 transform infrared spectroscopy (AFTIR), J. Geophys. Res.-Atmos. 105, 22147-22166, 2000.

609
610 Grieshop, A.P., Logue, J.M., Donahue, N.M. and Robinson, A.L.: Laboratory investigation of
611 photochemical oxidation of organic aerosol from wood fires 1: measurement and simulation of
612 organic aerosol evolution, Atmos. Chem. Phys. 9, 1263-1277, 2009a.

613
614 Grieshop, A.P., Donahue, N.M. and Robinson, A.L.: Laboratory investigation of photochemical
615 oxidation of organic aerosol from wood fires 2: analysis of aerosol mass spectrometer data,
616 Atmos. Chem. Phys. 9, 2227-2240, 2009b.

617
618 Guofeng, S., Siye, W., Wen, W., Yanyan, Z., Yujia, M., Bin, W., Rong, W., Wei, L., Huizhong,
619 S., Ye, H., Yifeng, Y., Wei, W., Xilong, W., Xuejun, W. and Shu, T.: Emission factors, size
620 distributions, and emission inventories of carbonaceous particulate matter from residential wood
621 combustion in rural China, Environ. Sci. Technol. 46, 4207-4214, 2012.

622

623 Hansson, K.-M., Samuelsson, J., Tullin, C. and Åmand, L.-E.: Formation of HNCO, HCN, and
624 NH$_3$ from the pyrolysis of bark and nitrogen-containing model compounds, Combust. Flame
625 137, 265-277, 2004.

626
627 Hedberg, E., Kristensson, A., Ohlsson, M., Johansson, C., Johansson, P.-Å., Swietlicki, E.,
628 Vesely, V., Wideqvist, U. and Westerholm, R.: Chemical and physical characterization of
629 emissions from birch wood combustion in a wood stove, Atmos. Environ. 36, 4823-4837, 2002.

630
631 Hennigan, C.J., Sullivan, A.P., Collett, J.L. and Robinson, A.L.: Levoglucosan stability in
632 biomass burning particles exposed to hydroxyl radicals, Geophys. Res. Lett. 37,
633 doi:10.1029/2010GL043088, 2010.

634
635 Herich, H., Gianini, M.F.D., Piot, C., Močnik, G., Jaffrezo, J.L., Besombes, J.L., Prévôt, A.S.H.
636 and Hueglin, C.: Overview of the impact of wood burning emissions on carbonaceous aerosols
637 and PM in large parts of the Alpine region, Atmos. Environ. 89, 64-75, 2014.

638
639 Heringa, M.F., DeCarlo, P.F., Chirico, R., Tritscher, T., Dommen, J., Weingartner, E., Richter,
640 R., Wehrle, G., Prévôt, A.S.H. and Baltensperger, U.: Investigations of primary and secondary
641 particulate matter of different wood combustion appliances with a high-resolution time-of-flight
642 aerosol mass spectrometer, Atmos. Chem. Phys. 11, 5945-5957, 2011.

643
644 Hobbs, P.V., Sinha, P., Yokelson, R.J., Christian, T.J., Blake, D.R., Gao, S., Kirchstetter, T.W.,
645 Novakov, T. and Pilewskie, P.: Evolution of gases and particles from a savanna fire in South
646 Africa, J. Geophys. Res.-Atmos. 108, doi:10.1029/2002JD002352, 2003.

647
648 Holzinger, R., Warneke, C., Hansel, A., Jordan, A., Lindinger, W., Scharffe, D.H., Schade, G.
649 and Crutzen, P.J.: Biomass burning as a source of formaldehyde, acetaldehyde, methanol,
650 acetone, acetonitrile, and hydrogen cyanide, Geophys. Res. Lett. 26, 1161-1164, 1999.

651
652 Holzinger, R., Williams, J., Salisbury, G., Klüpfel, T., de Reus, M., Traub, M., Crutzen, P.J. and
653 Lelieveld, J.: Oxygenated compounds in aged biomass burning plumes over the Eastern
654 Mediterranean: evidence for strong secondary production of methanol and acetone, Atmos.
655 Chem. Phys. 5, 39-46, 2005.

656
657 Ito, A. and Penner, J.E.: Global estimates of biomass burning emissions based on satellite
658 imagery for the year 2000, J. Geophys. Res.-Atmos. 109, doi:10.1029/2003JD004423, 2004.

659
660 Jordan, A., Haidacher, S., Hanel, G., Hartungen, E., Märk, L., Seehauser, H., Schottkowsky, R.,
661 Sulzer, P. and Märk, T.D.: A high resolution and high sensitivity proton-transfer-reaction time-
662 of-flight mass spectrometer (PTR-TOF-MS), Int. J. Mass. Spectrom. 286, 122-128, 2009.

663

664 Jordan, T.B. and Seen, A.J.: Effect of airflow setting on the organic composition of woodheater
665 emissions, Environ. Sci. Technol. 39, 3601-3610, 2005.

666

667 Jost, C., Trentmann, J., Sprung, D., Andreae, M.O., McQuaid, J.B. and Barjat, H.: Trace gas
668 chemistry in a young biomass burning plume over Namibia: Observations and model
669 simulations, J. Geophys. Res.-Atmos. 108, doi:10.1029/2002JD002431, 2003.

670

671 Kistler, M., Schmidl, C., Padouvas, E., Giebl, H., Lohninger, J., Ellinger, R., Bauer, H. and
672 Puxbaum, H.: Odor, gaseous and PM_{10} emissions from small scale combustion of wood types
673 indigenous to Central Europe, Atmos. Environ. 51, 86-93, 2012.

674

675 Krecl, P., Hedberg Larsson, E., Ström, J. and Johansson, C.: Contribution of residential wood
676 combustion and other sources to hourly winter aerosol in Northern Sweden determined by
677 positive matrix factorization, Atmos. Chem. Phys. 8, 3639-3653, 2008.

678

679 Kroll, J.H. and Seinfeld, J.H.: Chemistry of secondary organic aerosol: formation and evolution
680 of low-volatility organics in the atmosphere, Atmos. Environ. 42, 3593-3624, 2008.

681

682 Lindinger, W., Hansel, A. and Jordan, A.: On-line monitoring of volatile organic compounds at
683 pptv levels by means of proton-transfer-reaction mass spectrometry (PTR-MS) medical
684 applications, food control and environmental research, Int. J. Mass. Spectrom. 173, 191-241,
685 1998.

686

687 Mason, S.A., Field, R.J., Yokelson, R.J., Kochivar, M.A., Tinsley, M.R., Ward, D.E. and Hao,
688 W.M.: Complex effects arising in smoke plume simulations due to inclusion of direct emissions
689 of oxygenated organic species from biomass combustion, J. Geophys. Res.-Atmos. 106, 12527-
690 12539, 2001.

691

692 McDonald, J.D., Zielinska, B., Fujita, E.M., Sagebiel, J.C., Chow, J.C. and Watson, J.G.: Fine
693 particle and gaseous emission rates from residential wood combustion, Environ. Sci. Technol.
694 34, 2080-2091, 2000.

695

696 Midey, A.J., Williams, S., Miller, T.M. and Viggiano, A.A.: Reactions of O_2^+, NO^+ and H_3O^+
697 with methylcyclohexane (C_7H_{14}) and cyclooctane (C_8H_{16}) from 298 to 700 K, Int. J. Mass.
698 Spectrom. 222, 413-430, 2003.

699

700 Müller, M., Anderson, B.E., Beyersdorf, A.J., Crawford, J.H., Diskin, G.S., Eichler, P., Fried, A.,
701 Keutsch, F.N., Mikoviny, T., Thornhill, K.L., Walega, J.G., Weinheimer, A.J., Yang, M.,

702 Yokelson, R.J. and Wisthaler, A.: In situ measurements and modeling of reactive trace gases in a
703 small biomass burning plume, Atmos. Chem. Phys. 16, 3813-3824, 2016.

704
705 Nozière, B., Kalberer, M., Claeys, M., Allan, J., D'Anna, B., Decesari, S., Finessi, E., Glasius,
706 M., Grgić, I., Hamilton, J.F., Hoffmann, T., Iinuma, Y., Jaoui, M., Kahnt, A., Kampf, C.J.,
707 Kourtchev, I., Maenhaut, W., Marsden, N., Saarikoski, S., Schnelle-Kreis, J., Surratt, J.D.,
708 Szidat, S., Szmigielski, R. and Wisthaler, A.: The molecular identification of organic compounds
709 in the atmosphere: state of the art and challenges, Chem. Rev. 115, 3919-3983, 2015.

710
711 Overend, R. and Paraskevopoulos, G.: Rates of hydroxyl radical reactions. 4. Reactions with
712 methanol, ethanol, 1-propanol, and 2-propanol at 296 K, J. Phys. Chem. 82, 1329-1333, 1978.

713
714 Ozil, F., Tschamber, V., Haas, F. and Trouvé, G.: Efficiency of catalytic processes for the
715 reduction of CO and VOC emissions from wood combustion in domestic fireplaces, Fuel
716 Process. Technol. 90, 1053-1061, 2009.

717
718 Paraskevopoulou, D., Liakakou, E., Gerasopoulos, E. and Mihalopoulos, N.: Sources of
719 atmospheric aerosol from long-term measurements (5 years) of chemical composition in Athens,
720 Greece, Sci. Total Environ. 527–528, 165-178, 2015.

721
722 Paulot, F., Wunch, D., Crounse, J.D., Toon, G.C., Millet, D.B., DeCarlo, P.F., Vigouroux, C.,
723 Deutscher, N.M., González Abad, G., Notholt, J., Warneke, T., Hannigan, J.W., Warneke, C., de
724 Gouw, J.A., Dunlea, E.J., De Mazière, M., Griffith, D.W.T., Bernath, P., Jimenez, J.L. and
725 Wennberg, P.O.: Importance of secondary sources in the atmospheric budgets of formic and
726 acetic acids, Atmos. Chem. Phys. 11, 1989-2013, 2011.

727
728 Pettersson, E., Boman, C., Westerholm, R., Boström, D. and Nordin, A.: Stove performance and
729 emission characteristics in residential wood log and pellet combustion, part 2: wood stove,
730 Energ. Fuel 25, 315-323, 2011.

731
732 Platt, S.M., El Haddad, I., Zardini, A.A., Clairotte, M., Astorga, C., Wolf, R., Slowik, J.G.,
733 Temime-Roussel, B., Marchand, N., Ježek, I., Drinovec, L., Močnik, G., Möhler, O., Richter, R.,
734 Barmet, P., Bianchi, F., Baltensperger, U. and Prévôt, A.S.H.: Secondary organic aerosol
735 formation from gasoline vehicle emissions in a new mobile environmental reaction chamber,
736 Atmos. Chem. Phys. 13, 9141-9158, 2013.

737
738 Pouli, A.E., Hatzinikolaou, D.G., Piperi, C., Stavridou, A., Psallidopoulos, M.C. and Stavrides,
739 J.C.: The cytotoxic effect of volatile organic compounds of the gas phase of cigarette smoke on
740 lung epithelial cells, Free Radical Bio. Med. 34, 345-355, 2003.

741

Praplan, A.P., Hegyi-Gaeggeler, K., Barmet, P., Pfaffenberger, L., Dommen, J. and Baltensperger, U.: Online measurements of water-soluble organic acids in the gas and aerosol phase from the photooxidation of 1,3,5-trimethylbenzene, Atmos. Chem. Phys. 14, 8665-8677, 2014.

Reda, A.A., Czech, H., Schnelle-Kreis, J., Sippula, O., Orasche, J., Weggler, B., Abbaszade, G., Arteaga-Salas, J.M., Kortelainen, M., Tissari, J., Jokiniemi, J., Streibel, T. and Zimmermann, R.: Analysis of gas-phase carbonyl compounds in emissions from modern wood combustion appliances: influence of wood type and combustion appliance, Energ. Fuel 29, 3897-3907, 2015.

Sato, K., Hatakeyama, S. and Imamura, T.: Secondary organic aerosol formation during the photooxidation of toluene: NO_x dependence of chemical composition, J. Phys. Chem. A 111, 9796-9808, 2007.

Schauer, J.J., Kleeman, M.J., Cass, G.R. and Simoneit, B.R.T.: Measurement of emissions from air pollution sources. 3. C_1-C_{29} organic compounds from fireplace combustion of wood, Environ. Sci. Technol. 35, 1716-1728, 2001.

Schmidl, C., Luisser, M., Padouvas, E., Lasselsberger, L., Rzaca, M., Ramirez-Santa Cruz, C., Handler, M., Peng, G., Bauer, H. and Puxbaum, H.: Particulate and gaseous emissions from manually and automatically fired small scale combustion systems, Atmos. Environ. 45, 7443-7454, 2011.

Shao, M., Lu, S., Liu, Y., Xie, X., Chang, C., Huang, S. and Chen, Z.: Volatile organic compounds measured in summer in Beijing and their role in ground-level ozone formation, J. Geophys. Res.-Atmos. 114, doi:10.1029/2008JD010863, 2009.

Singh, H.B., Salas, L., Herlth, D., Kolyer, R., Czech, E., Viezee, W., Li, Q., Jacob, D.J., Blake, D., Sachse, G., Harward, C.N., Fuelberg, H., Kiley, C.M., Zhao, Y. and Kondo, Y.: In situ measurements of HCN and CH_3CN over the Pacific Ocean: Sources, sinks, and budgets, J. Geophys. Res.-Atmos. 108, doi:10.1029/2002JD003006, 2003.

Singh, H.B., Salas, L.J., Chatfield, R.B., Czech, E., Fried, A., Walega, J., Evans, M.J., Field, B.D., Jacob, D.J., Blake, D., Heikes, B., Talbot, R., Sachse, G., Crawford, J.H., Avery, M.A., Sandholm, S. and Fuelberg, H.: Analysis of the atmospheric distribution, sources, and sinks of oxygenated volatile organic chemicals based on measurements over the Pacific during TRACE-P, J. Geophys. Res.-Atmos. 109, doi:10.1029/2003JD003883, 2004.

IPCC: Climate Change 2013: The Physical Science Basis. Contribution of Working Group I to the Fifth Assessment Report of the Intergovernmental Panel on Climate Change, edited by:

782 Stocker, T.F., D. Qin, G.-K.P., M. Tignor, S. K. Allen, J. Boschung, A. Nauels, Y. Xia, V. Bex
783 and Midgley, P.M., Cambridge University Press, Cambridge, UK and New York, USA, 2013.

784
785 Stockwell, C.E., Veres, P.R., Williams, J. and Yokelson, R.J.: Characterization of biomass
786 burning emissions from cooking fires, peat, crop residue, and other fuels with high-resolution
787 proton-transfer-reaction time-of-flight mass spectrometry, Atmos. Chem. Phys. 15, 845-865,
788 2015.

789
790 Šyc, M., Horák, J., Hopan, F., Krpec, K., Tomšej, T., Ocelka, T. and Pekárek, V.: Effect of fuels
791 and domestic heating appliance types on emission factors of selected organic pollutants, Environ.
792 Sci. Technol. 45, 9427-9434, 2011.

793
794 Tabazadeh, A., Yokelson, R.J., Singh, H.B., Hobbs, P.V., Crawford, J.H. and Iraci, L.T.:
795 Heterogeneous chemistry involving methanol in tropospheric clouds, Geophys. Res. Lett. 31,
796 doi:10.1029/2003GL018775, 2004.

797
798 Tao, J., Gao, J., Zhang, L., Zhang, R., Che, H., Zhang, Z., Lin, Z., Jing, J., Cao, J. and Hsu, S.C.:
799 $PM_{2.5}$ pollution in a megacity of southwest China: source apportionment and implication, Atmos.
800 Chem. Phys. 14, 8679-8699, 2014.

801
802 Warneke, C., de Gouw, J.A., Kuster, W.C., Goldan, P.D. and Fall, R.: Validation of atmospheric
803 VOC measurements by proton-transfer-reaction mass spectrometry using a gas-chromatographic
804 preseparation method, Environ. Sci. Technol. 37, 2494-2501, 2003.

805
806 Warneke, C., de Gouw, J.A., Stohl, A., Cooper, O.R., Goldan, P.D., Kuster, W.C., Holloway,
807 J.S., Williams, E.J., Lerner, B.M., McKeen, S.A., Trainer, M., Fehsenfeld, F.C., Atlas, E.L.,
808 Donnelly, S.G., Stroud, V., Lueb, A. and Kato, S.: Biomass burning and anthropogenic sources
809 of CO over New England in the summer 2004, J. Geophys. Res.-Atmos. 111,
810 doi:10.1029/2005JD006878, 2006.

811
812 Warneke, C., Roberts, J.M., Veres, P., Gilman, J., Kuster, W.C., Burling, I., Yokelson, R. and de
813 Gouw, J.A.: VOC identification and inter-comparison from laboratory biomass burning using
814 PTR-MS and PIT-MS, Int. J. Mass. Spectrom. 303, 6-14, 2011.

815
816 Yokelson, R.J., Bertschi, I.T., Christian, T.J., Hobbs, P.V., Ward, D.E. and Hao, W.M.: Trace
817 gas measurements in nascent, aged, and cloud-processed smoke from African savanna fires by
818 airborne Fourier transform infrared spectroscopy (AFTIR), J. Geophys. Res.-Atmos. 108,
819 doi:10.1029/2002JD002322, 2003.

820

821   Yokelson, R.J., Christian, T.J., Karl, T.G. and Guenther, A.: The tropical forest and fire
822   emissions experiment: laboratory fire measurements and synthesis of campaign data, Atmos.
823   Chem. Phys. 8, 3509-3527, 2008.

824
825   Yokelson, R.J., Crounse, J.D., DeCarlo, P.F., Karl, T., Urbanski, S., Atlas, E., Campos, T.,
826   Shinozuka, Y., Kapustin, V., Clarke, A.D., Weinheimer, A., Knapp, D.J., Montzka, D.D.,
827   Holloway, J., Weibring, P., Flocke, F., Zheng, W., Toohey, D., Wennberg, P.O., Wiedinmyer,
828   C., Mauldin, L., Fried, A., Richter, D., Walega, J., Jimenez, J.L., Adachi, K., Buseck, P.R., Hall,
829   S.R. and Shetter, R.: Emissions from biomass burning in the Yucatan, Atmos. Chem. Phys. 9,
830   5785-5812, 2009.

831
832   Zhang, X., Cappa, C.D., Jathar, S.H., McVay, R.C., Ensberg, J.J., Kleeman, M.J. and Seinfeld,
833   J.H.: Influence of vapor wall loss in laboratory chambers on yields of secondary organic aerosol,
834   Proceedings of the National Academy of Sciences 111, 5802–5807, 2014.

835

836

Table 1. Modified combustion efficiencies, OH exposures of reported aged values (molec cm^{-3} h) and enhancement of select species relative to CO enhancement above background levels (pptv ppbv^{-1})

parameter	experiment					average[a]
	1	2	3	4	5	
MCE	0.975	0.978	0.977	0.974	0.978	0.976±0.002
OH exposure	4.5×10^7	5.5×10^7	5.3×10^7	5.2×10^7	4.7×10^7	-
$\Delta CH_3CN_{primary}/\Delta CO$	0.079	0.11	0.099	0.077	0.082	0.09±0.01
$\Delta CH_3CN_{aged}/\Delta CO$	0.084	0.11	0.11	0.072	0.069	0.09±0.02
$\Delta CH_3OH_{primary}/\Delta CO$	3.4	21	11	2.4	1.5	8±8
$\Delta CH_3OH_{aged}/\Delta CO$	3.4	19	11	2.5	1.8	7±7
$\Delta C_2H_4O_{2primary}/\Delta CO$	12	84	57	9.8	5.9	30±30
$\Delta C_2H_4O_{2aged}/\Delta CO$	12	68	48	9.4	6.5	30±30

[a]Uncertainties correspond to one sample standard deviation of the replicates.

Table 2. Primary emission factors of gas-phase species (mg kg^{-1})[a,b]

species	monoisotopic m/z	structural assignment[c]	functional group	experiment 1	2	3	4	5	average[d]
CO_2				1780000	1781000	1777000	1772000	1784000	1779000 ±4000
CO				27000	26000	27000	30000	27000	28000±2000
CH_4				1800	1600	2000	2800	1500	1900±500
NMOG				2800	13000	9200	3200	1500	6000±5000
acid				750	5000	3500	700	340	2000±2000
O-containing				560	3400	2200	590	290	1000±1000
carbonyl				310	1500	960	270	170	600±600
oxygenated aromatic				230	780	520	270	140	400±300
alcohol				130	660	360	90	48	300±300
furan				93	680	410	95	51	300±300
O- and N-containing				120	81	77	120	91	100±20
C_xH_y				120	210	210	160	64	150±60
aromatic hydrocarbon				320	170	490	680	250	400±200
N-containing				20	39	36	23	16	30±10
other				140	390	310	160	94	200±100
$[CH_3OH+H]^+$	33.034	methanol	alcohol	110	660	360	87	47	300±300
$[C_2H_3N+H]^+$	42.034	acetonitrile	N-containing	3.4	3.4	4.1	3.6	3.2	3.5±0.3
$[C_3H_6+H]^+$	43.055	propene	C_xH_y	38	61	40	28	15	40±20
$[C_2H_4O+H]^+$	45.034	acetaldehyde	carbonyl	94	330	230	79	48	200±100
$[CH_2O_2+H]+$	47.013	formic acid	acid	9.9	96	100	31	4.2	50±50
$[C_2H_6O+H]^+$	47.050	ethanol	alcohol	16	BDL	3.3	2.5	BDL	4±7
$[C_4H_6+H]^+$	55.055	buta-1,3-diene	C_xH_y	14	38	33	14	5.7	20±10
$[C_3H_4O+H]^+$	57.034	prop-2-enal	carbonyl	45	160	120	45	25	80±60
$[C_2H_2O_2+H]^+$	59.013	oxaldehyde	carbonyl	BDL	BDL	BDL	1.3	BDL	0.3±0.6
$[C_3H_6O+H]^+$	59.050	propan-2-one propanal	carbonyl	54	190	120	30	30	80±70
$[C_2H_4O_2+H]^+$	61.029	acetic acid glycolaldehyde	acid	740	4900	3400	670	340	2000±2000
$[C_4H_4O+H]^+$	69.034	furan	furan	17	140	82	19	9.7	50±60
$[C_5H_8+H]^+$	69.070	isoprene cyclopentene	C_xH_y	3.4	12	9.4	2.8	1.1	3±2
$[C_4H_6O+H]^+$	71.050	(E)-but-2-enal 3-buten-2-one 2-methylprop-2-enal	carbonyl	25	120	72	19	14	50±40
$[C_5H_{10}+H]^+$	71.086	(E)-/(Z)-pent-2-ene 2-methylbut-1-ene 2-methylbut-2-ene pent-1-ene 3-methylbut-1-ene	C_xH_y	2.7	5.3	4.0	2.0	0.86	3±2
$[C_3H_4O_2+H]^+$	73.029	2-oxopropanal	carbonyl	26	140	96	26	15	60±50
$[C_4H_8O+H]^+$	73.065	butan-2-one butanal 2-methylpropanal	carbonyl	7.2	44	24	5.2	4.2	20±20
$[C_3H_6O_2+H]^+$	75.045	methyl acetate	O-containing	62	490	300	56	28	200±200
$[C_6H_6+H]^+$	79.055	benzene	aromatic hydrocarbon	210	90	300	450	150	200±100
$[C_5H_6O+H]^+$	83.050	2-methylfuran	furan	21	160	88	21	12	60±60
$[C_5H_8O+H]^+$	85.065	3-methyl-3-buten-2-one	carbonyl	10	69	39	8.7	5.4	30±30
$[C_6H_{12}+H]^+$	85.102	(E)-hex-2-ene 2-methyl-pent-2-ene	C_xH_y	BDL	2.2	1.6	0.60	BDL	1±1
$[C_4H_6O_2+H]^+$	87.045	butane-2,3-dione	carbonyl	51	450	250	52	26	200±200
$[C_7H_8+H]^+$	93.070	toluene	aromatic hydrocarbon	23	22	34	39	16	27±9
$[C_6H_6O+H]^+$	95.050	phenol	oxygenated aromatic	110	110	130	130	68	110±20
$[C_5H_4O_2+H]^+$	97.029	furan-2-carbaldehyde	furan	40	270	180	40	21	100±100
$[C_6H_8O+H]^+$	97.065	2,4-/2,5-dimethylfuran	furan	11	86	48	11	5.5	30±30
$[C_4H_2O_3+H]^+$	99.008	maleic anhydride[e]	O-containing	40	91	66	40	26	50±30
$[C_8H_8+H]^+$	105.070	styrene	aromatic hydrocarbon	12	8.0	20	24	9.6	15±7
$[C_7H_6O+H]^+$	107.050	benzaldehyde	oxygenated aromatic	18	14	23	27	11	18±7
$[C_8H_{10}+H]^+$	107.086	m-/o-/p-xylene ethylbenzene	aromatic hydrocarbon	4.2	6.9	7.5	6.3	2.9	6±2
$[C_7H_8O+H]^+$	109.065	m-/o-/p-cresol	oxygenated aromatic	24	71	48	25	14	40±20
$[C_6H_6O_2+H]^+$	111.045	m-/o-/p-benzenediol 2-methylfuraldehyde	oxygenated aromatic	26	150	86	22	14	60±50
$[C_9H_8+H]^+$	117.070	1H-indene	aromatic hydrocarbon	5.0	BDL	9.5	15	2.9	6±6
$[C_9H_{10}+H]^+$	119.086	2,3-dihydro-1H-indene	aromatic	2.3	2.8	3.9	3.3	1.3	3±1

44

			hydrocarbon						
$[C_8H_8O+H]^+$	121.065	1-phenylethanone 3-/4-methylbenzaldehyde	oxygenated aromatic	8.3	14	13	8.8	4.6	10±4
$[C_9H_{12}+H]^+$	121.102	i-propylbenzene n-propylbenzene 1,3,5-trimethylbenzene	aromatic hydrocarbon	1.0	2.4	2.3	1.2	0.68	1.5±0.8
$[C_8H_{10}O+H]^+$	123.081	2,4-/2,6-/3,5-dimethylphenol	oxygenated aromatic	4.7	36	18	4.9	3.0	10±10
$[C_7H_8O_2+H]^+$	125.060	2-methoxyphenol methylbenzenediols	oxygenated aromatic	9.2	110	55	12	4.9	40±50
$[C_6H_6O_3+H]^+$	127.040	5-(hydroxymethyl)furan-2-carbaldehyde	furan	4.4	29	17	4.9	2.7	10±10
$[C_{10}H_8+H]^+$	129.070	naphthalene	aromatic hydrocarbon	42	20	80	100	33	60±30
$[C_8H_{10}O_2+H]^+$	139.076	2-methoxy-4-methylphenol 4-(2-hydroxyethyl)phenol	oxygenated aromatic	3.2	59	29	6.2	1.8	20±20
$[C_{11}H_{10}+H]^+$	143.086	1-/2-methylnaphthalene	aromatic hydrocarbon	4.0	2.3	5.7	7.5	3.3	5±2
$[C_9H_6O_2+H]^+$	147.045	2,3-dihydroinden-1-one	oxygenated aromatic	11	13	13	11	6.0	11±3
$[C_8H_4O_3+H]^+$	149.024	phthalic anhdyride[e]	O-containing	16	31	25	16	8.3	19±9
$[C_8H_8O_3+H]^+$	153.055	4-hydroxy-3-methoxybenzaldehyde	oxygenated aromatic	3.8	27	15	3.7	1.4	10±10
$[C_{12}H_8+H]^+$	153.070	acenaphthylene	aromatic hydrocarbon	6.1	3.6	12	15	8.3	9±5
$[C_9H_{12}O_2+H]^+$	153.092	4-ethyl-2-methoxyphenol 1,2-dimethoxy-4-methylbenzene	oxygenated aromatic	1.4	30	14	3.2	BDL	10±10
$[C_8H_{10}O_3+H]^+$	155.071	2,6-dimethoxyphenol	oxygenated aromatic	2.2	73	35	7.8	1.0	20±30
$[C_{12}H_{10}+H]^+$	155.086	1,1'-biphenyl 1,2-dihydroacenaphthylene	aromatic hydrocarbon	3.1	BDL	4.3	6.1	2.9	3±2
$[C_{12}H_{12}+H]^+$	157.102	dimethylnaphthalene	aromatic hydrocarbon	1.3	3.0	3.2	2.2	1.2	2.2±0.9
$[C_{10}H_{12}O_2+H]^+$	165.092	2-methoxy-4-[(E)-prop-1-enyl]phenol 2-methoxy-4-prop-2-enylphenol 2-methoxy-4-[(Z)-prop-1-enyl]phenol	oxygenated aromatic	0.92	24	13	2.3	0.59	8±10
$[C_9H_{10}O_3+H]^+$	167.071	1-(4-hydroxy-3-methoxyphenyl)ethanone 2,5-dimethylbenzaldehyde 3,4-dimethoxybenzaldehyde	oxygenated aromatic	2.5	11	6.7	2.2	1.2	5±4
$[C_{13}H_{10}+H]^+$	167.086	fluorene	aromatic hydrocarbon	BDL	BDL	1.0	2.5	2.0	1±1
$[C_{10}H_{14}O_2+H]^+)$	167.107	2-methoxy-4-propylphenol	oxygenated aromatic	0.88	7.6	4.4	1.1	BDL	3±3
$[C_9H_{12}O_3+H]^+$	169.086	2,6-dimethoxy-4-methylphenol	oxygenated aromatic	BDL	14	6.2	1.1	BDL	4±6
$[C_{14}H_{10}+H]^+$	179.086	phenanthrene anthracene	aromatic hydrocarbon	6.4	8.4	6.1	3.6	7.7	6±2
$[C_{13}H_8O+H]^+$	181.065	fluoren-9-one phenalen-1-one	oxygenated aromatic	2.7	4.0	2.7	1.2	1.9	2±1
$[C_{10}H_{12}O_3+H]^+$	181.086	1-(4-hydroxy-3-methoxyphenyl)propan-2-one	oxygenated aromatic	BDL	4.2	2.6	1.1	0.69	2±2
$[C_9H_{10}O_4+H]^+$	183.066	3,4-dimethoxybenzoic acid 4-hydroxy-3,5-dimethoxybenzaldehyde	oxygenated aromatic	1.1	BDL	1.4	1.1	1.0	0.9±0.5
$[C_{10}H_{14}O_3+H]^+$	183.102	4-ethyl-2,6-dimethoxyphenol	oxygenated aromatic	1.0	7.4	4.2	1.0	BDL	3±3
$[C_{15}H_{12}+H]^+$	193.102	1-/2-/3-/9-methylphenanthrene 2-methylanthracene	aromatic hydrocarbon	0.50	2.6	1.3	BDL	0.44	1±1
$[C_{11}H_{14}O_3+H]^+$	195.102	1,3-dimethoxy-2-prop-2-enoxybenzene 2,6-dimethoxy-4-[(Z)-prop-1-enyl]phenol	oxygenated aromatic	BDL	1.7	1.2	BDL	BDL	0.6±0.8
$[C_{16}H_{10}+H]^+$	203.086	fluoranthene pyrene acephenanthrylene	aromatic hydrocarbon	BDL	0.87	BDL	BDL	BDL	0.2±0.4

[a]CO_2, CO and CH_4 are measured using cavity ring down spectroscopy and all other species are measured using the PTR-ToF-MS.
[b]BDL indicates value is below the detection limit.
[c]Multiple structural assignments for a given ion correspond to possible isomers.
[d]Uncertainties correspond to one sample standard deviation of the replicates.
[e]Structural assignment based on known products produced during oxidation of aromatics
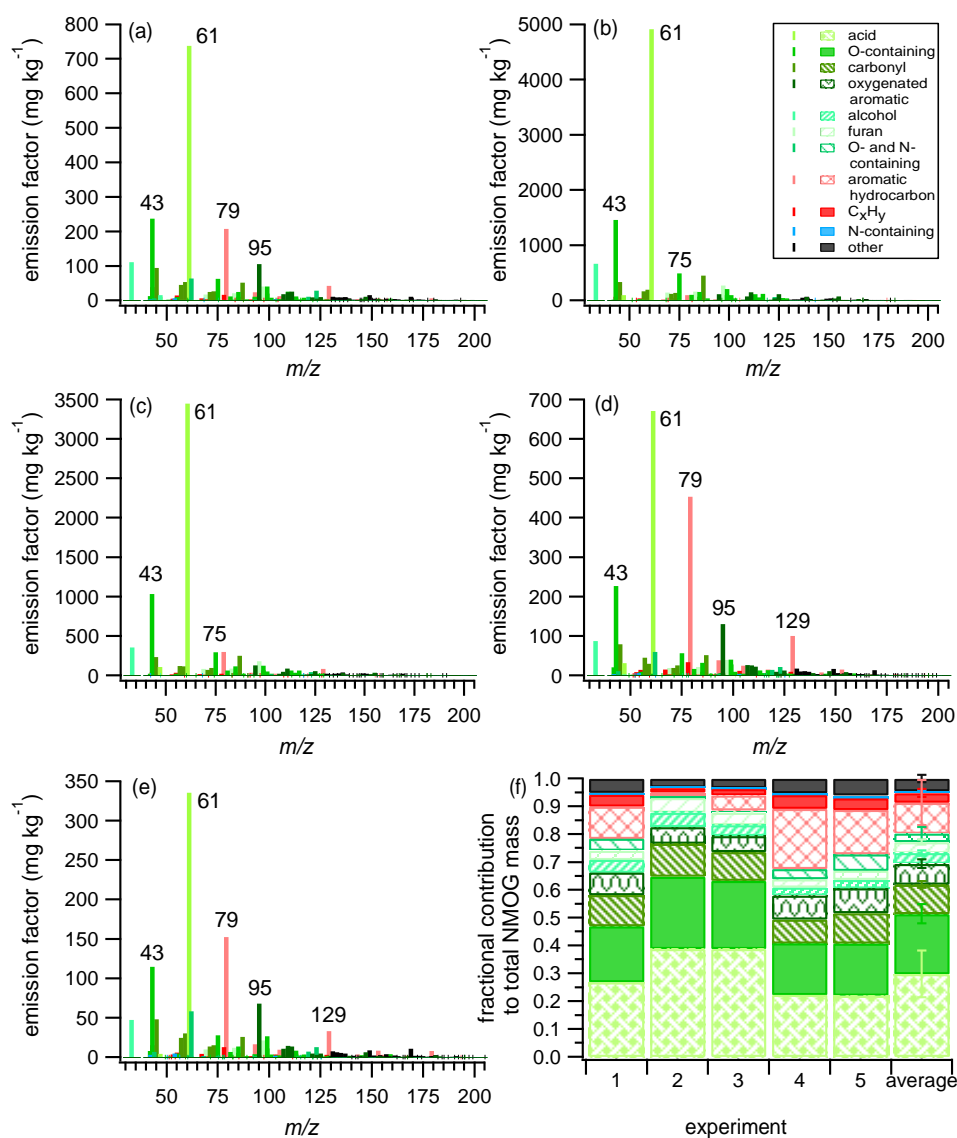(Bandow et al., 1985; Chan et al., 2009; Praplan et al., 2014).

Figure 1. Mass spectra of primary emissions for experiments 1-5 (a-e) colored by functional group. (a-e) Labelled peaks correspond to $[C_2H_3O]^+$ (*m/z* 43, fragment from higher molecular weight compounds), $[C_2H_4O_2+H]^+$ (*m/z* 61, acetic acid), $[C_3H_6O_2+H]^+$ (*m/z* 75, methyl acetate), $[C_6H_6+H]^+$ (*m/z* 79, benzene), $[C_6H_6O+H]^+$ (*m/z* 95, phenol) and $[C_{10}H_8+H]^+$ (*m/z* 129, naphthalene). The bars in (f) correspond to the fractional contribution of each functional group to the total NMOG mass for each experiment and the average of all experiments. Error bars correspond to one sample standard deviation of the replicates. Legend in (b) applies to (a-f).
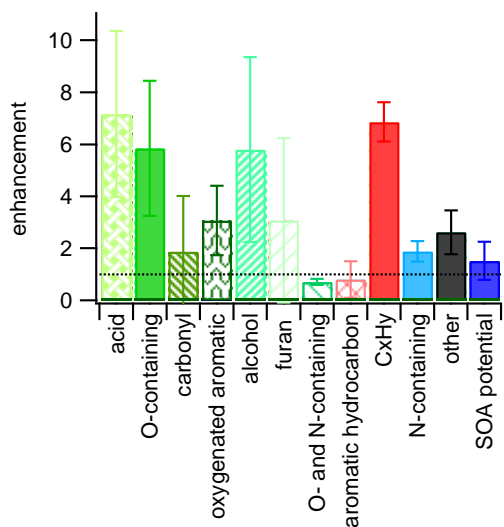
Figure 2. Enhancement (average value (mg kg^{-1}) of experiments 2 and 3 relative to the average value of experiments 1, 4 and 5) in each NMOG functional group category and for SOA formation potential. Total SOA formation potential is determined using the primary EF of each NMOG identified as a SOA precursor and literature SOA yields and assumes complete consumption of each NMOG with aging (see text for details). Error bars correspond to one sample standard deviation.
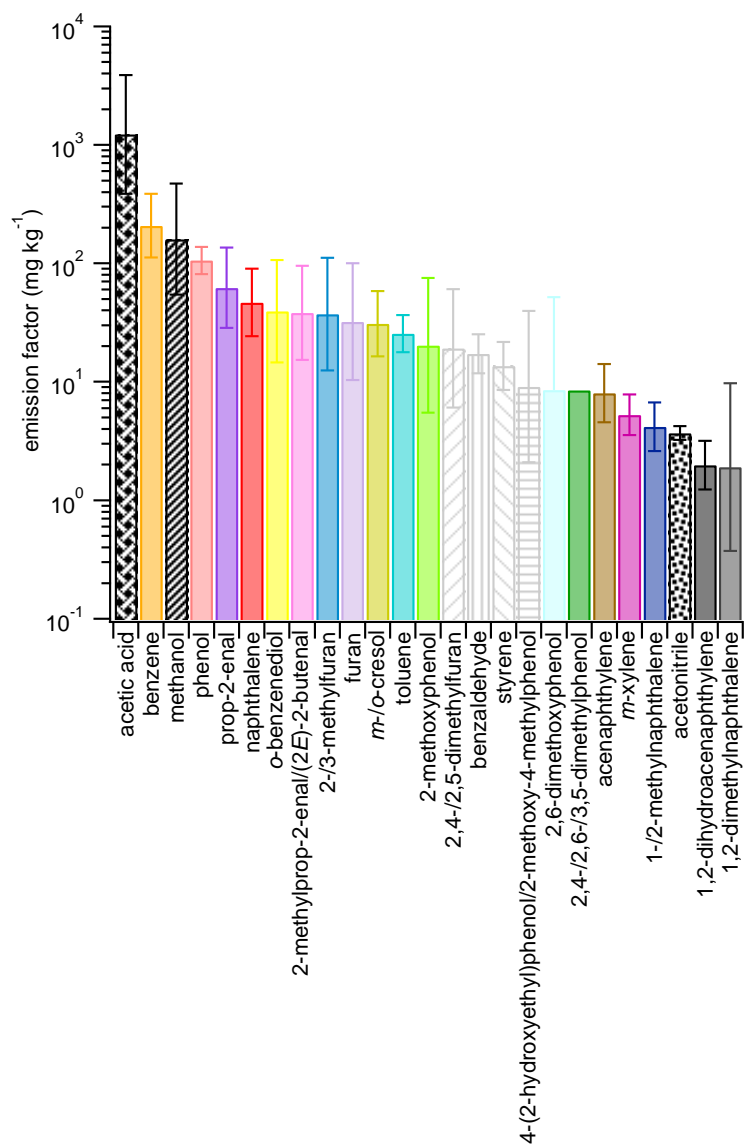
Figure 3. Geometric mean of the primary emission factors for gas-phase species of particular interest for SOA formation (solid bars and gray patterned bars) and identification of air masses influenced by biomass burning (black patterned bars). Colors and patterns corresponding to NMOGs contributing to SOA formation are consistent with Bruns et al. (2016). Error bars correspond to the sample geometric standard deviation of the replicates.
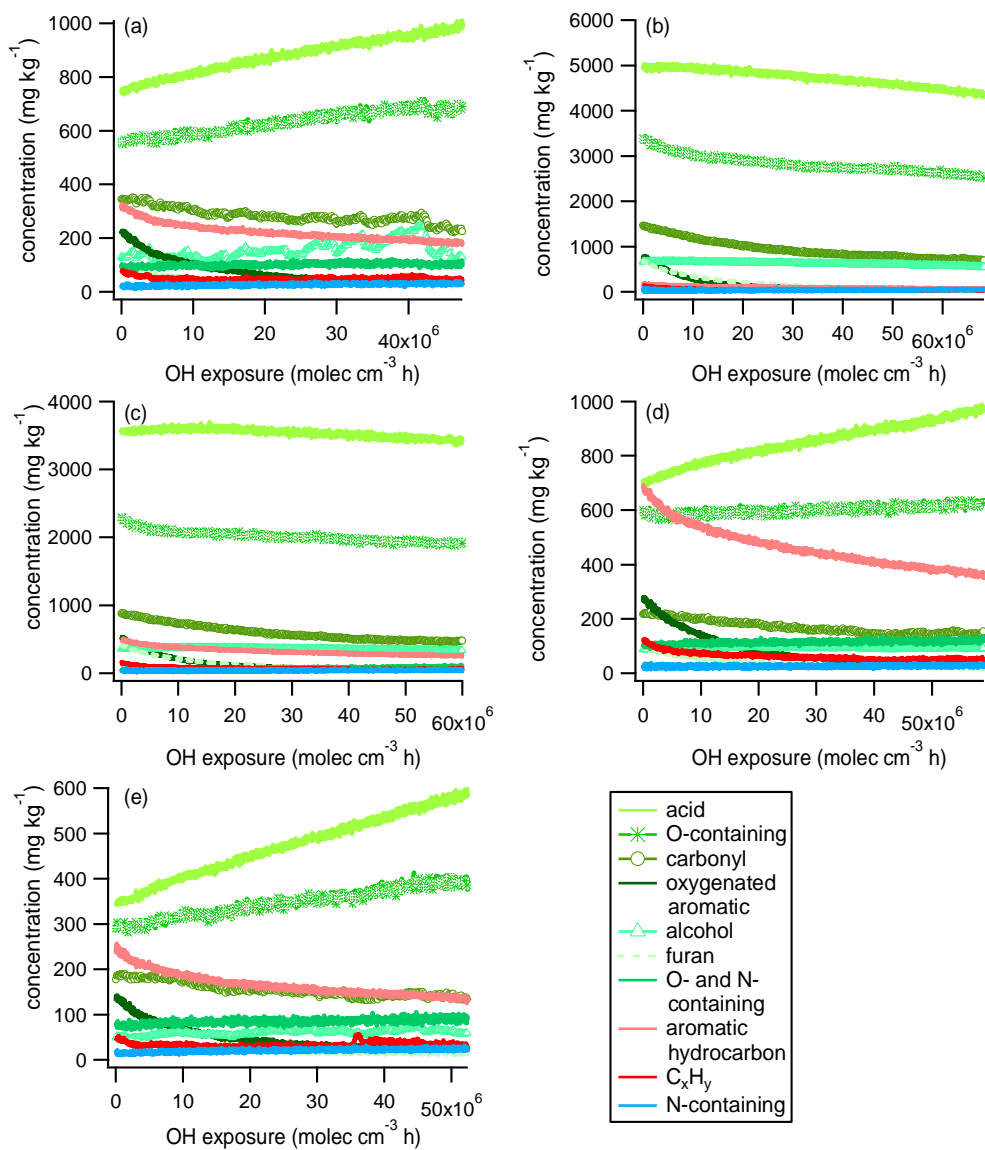
Figure 4. (a-e) Temporal evolution of gas-phase species categorized by functional group throughout aging in the smog chamber for experiments 1-5 (a-e). Units on the y-axes are mass of each functional group (mg) per mass of wood consumed (kg).
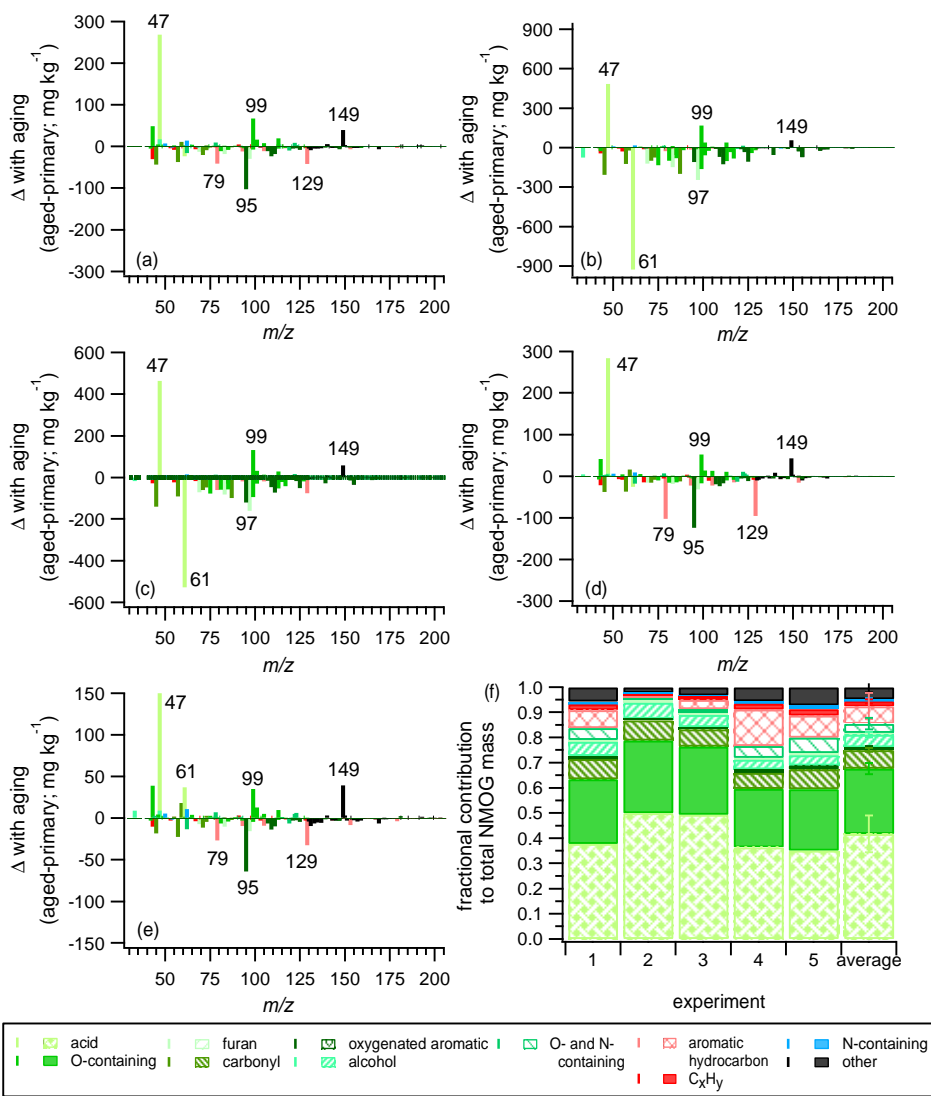
Figure 5. Absolute difference of aged and primary mass spectra for experiments 1-5 (a-e), where peaks less than zero decrease during aging and peaks greater than zero increase during aging. Aged emissions correspond to an OH exposure of $(4.5\text{-}5.5)\times10^7$ molec cm^{-3} h. (a-e) Labelled peaks correspond to $[CH_2O_2+H]^+$ (*m/z* 47, formic acid), $[C_2H_4O_2+H]^+$ (*m/z* 61, acetic acid), $[C_6H_6+H]^+$ (*m/z* 79, benzene), $[C_6H_6O+H]^+$ (*m/z* 95, phenol), $[C_5H_4O_2+H]^+$ (*m/z* 97, furan-2-carbaldehyde), $[C_4H_2O_3+H]^+$ (*m/z* 99, maleic anhydride), $[C_{10}H_8+H]^+$ (*m/z* 129, naphthalene) and $[C_8H_4O_3+H]^+$ (*m/z* 149, phthalic anhydride). The bars in (f) correspond to the fractional contribution of each category to the total NMOG EF at an OH exposure of $(4.5\text{-}5.5)\times10^7$ molec cm^{-3} h for each experiment and the average of all experiments. Error bars correspond to one sample standard deviation of the replicates.